2004 CEDAR Workshop
Eldorado Hotel
Santa Fe, New Mexico, USA
June 27 - July 2, 2004

Poster Sessions Booklet

June 29-30

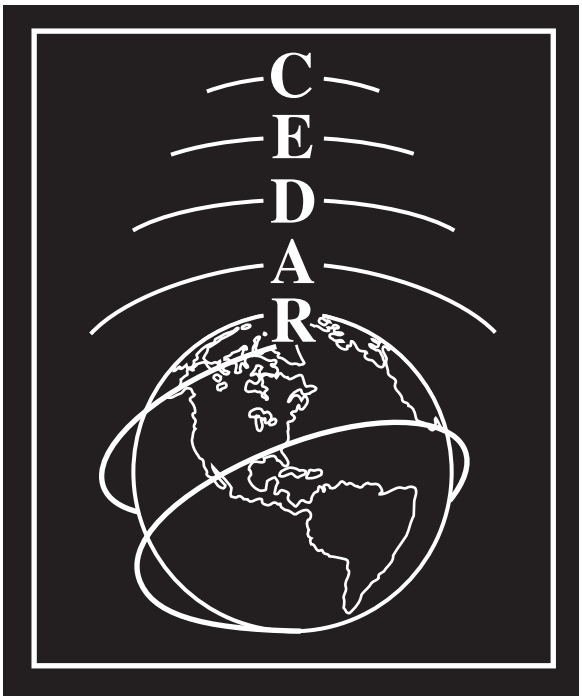

Sponsored by HAO/NCAR and NSF

Contents

1 Tuesday Evening 29 June 2004 Poster Session Abstracts, Data visualization and management

1.1 VIZ.01: Space Physics Metadata Searching Using Space Physics Data Markup Language (SPDML) – by Weiss, Michele

Status of First Author: Nonstudent

Authors: Michele Weiss, JHU/APL, michele.weiss@jhuapl.edu Daniel Morrison, JHU/APL, daniel.morrision@jhuapl.edu, Mohammed Hashemian, JHU/APL, mohammed.hashemian@jhuapl.edu, Robin Barnes, JHU/APL, robin.barnes@jhuapl.edu, Larry Paxton, JHU/APL, larry.paxton@jhuapl.edu

Abstract: The Space Physics Data Markup Language (SPDML) defines an eXtensible Markup Language (XML) for expressing Space Physics Metadata. The purpose is to develop an extensible standard for next generation multi-mission catalog searching capabilities such as those proposed for use in Virtual Observatories. SPDML provides a standard method for expressing Space Physics metadata and is being utilized in a prototype system that provides a standard method of data querying enabling multi-instrument comparison to TIMED data and tracing the Sun-Earth connection. SPDML is using a data dictionary that is compatible with the developing Space Physics Archive Search and Extract (SPASE) data dictionary. A testbed is being developed using data from the NASA TIMED spacecraft and ground-based SuperDARN radars to demonstrate the multi-mission search capabilities (http://sd-www.jhuapl.edu/SPDML). Examples from this testbed will be presented.

1.2 VIZ.02: SPASE - The Space Physics Archive Search and Exchange: Finding and Accessing Data – by Thieman, James presented by Weiss, Michele

Status of First Author: Nonstudent

Authors: James Thieman, NASA/GSFC thieman@nssdc.gsfc.nasa.gov Michele Weiss, JHU/APL michele.weiss@jhuapl.edu Aaron Roberts, NASA/GSFC roberts@vayu.gsfc.nasa.gov Todd King, UCLA/IGPP tking@igpp.ucla.edu

Abstract: The Space Physics Archive Search and Exchange (SPASE) is a collaborative development effort among multi-institution, international, space physics data holding organizations intended to allow science users to find space physics data of interest, intercompare the data, and retrieve selected data sets or portions of data sets. The search would be done across multiple data centers through a single search initiated through a network accessible interface. The effort involves creation of a common space physics data model and development of an intermediate level of software that will translate queries into the search mechanisms specific to each of the data centers. The results of the search are then to be put into a common format to present to the user. Thus, there is no need to change the software and search procedures used at the individual data holding institutions. Metadata entry tools are planned to ease the translation of the metadata to be found at the archive locations to the common metadata format needed for the SPASE searching. Data set intercomparison tools will enable determination of which data sets or portions of data sets are useful for the purposes of the scientist/user and need to be requested from the data provider. The present status of the efforts and plans for the future will be discussed. We welcome discussion of the needs of the CEDAR community and how to assure fulfillment of those needs.

1.3 VIZ.03: Ionosphere Models at the Community Coordinated Modeling Center. – by Kuznetsova, Maria

Status of First Author: Nonstudent

Authors: M. Kuznetsova,, M. Hesse, L. Rastaetter, A. Narock, K. Keller, M. Maddox

Abstract: The Community Coordinated Modeling Center (CCMC) is offering runs on request of space weather models residing at CCMC to a broad space science community. Runs on request support an open model policy by providing community access to state-of-the-art research models. They also facilitate model testing by a large number of researches. We will present an overview of models residing at CCMC, demonstrate how to use these models, how to analyze model results, and discuss future plans for ionosphere/thermosphere models. CCMC solicits input on how to further improve customer service to the research community.

1.4 VIZ.04: Accessing the Madrigal Database via Web Services – by Rideout, William

Status of First Author: Nonstudent

Authors: William Rideout, MIT Haystack Observatory, brideout@haystack,mit.edu John Holt, MIT Haystack Observatory, jmh@haystack,mit.edu

Abstract: With the release of Madrigal 2.3, Madrigal now exposes all the information and capabilities it has as web services. This new feature allows easy access to Madrigal from any computer on the Internet using any platform (Unix, Windows, Mac, etc) and almost any programming language. The basic concept of web services is to use the existing world wide web infrastructure to expose a standard programmatic interface instead of a user interface. This means that a user can now access Madrigal data from within any program they write in any programming language; they do not need to use our web interface. Madrigal's web services are basically cgi scripts with simple output that allows easy parsing of the information. Any language that supports the HTTP standard can then access any Madrigal site. We have written and will demonstrate remote API's using python and Matlab, but almost any language can be used. The use of web services can play an important role in standardizing the way scientific data can be accessed by the community.

1.5 VIZ.05: Road map of the TIMED Science Data System web site – by Nylund, Stuart

Status of First Author: Nonstudent

Authors: Stuart Nylund, JHU/APL, stuart.nylund@jhuapl.edu Paul Lafferty, JHU/APL, paul.lafferty@jhuapl.edu

Abstract: The Thermosphere Ionosphere Mesosphere Energetics and Dynamics (TIMED) Science Data System (SDS) is the distributed system responsible for the acquisition, generation, distribution, and archive of science data necessary to support the TIMED mission. The SDS provides a single user interface, implemented as a World Wide Web (Web) site, for TIMED investigators, the scientific community and the general public to locate, understand and use its collection of data - now continuously covering over 29 months. The SDS integrates resources dispersed across several different facilities: a Mission Data Center (MDC) - the facility responsible for telemetry distribution and other central functions; and four instrument Payload Operations Centers (POC) - remote facilities responsible for TIMED instrument data operations of data reduction, processing and distribution of data analysis products. Additionally, through support furnished primarily by CEDAR, collaborating ground-based investigators make data available through the SDS.
The major features of the TIMED SDS Web site for coordinated observation planning, information access, and data query and retrieval are presented. Illustrations show how to navigate and use the various resources of the site. Example results are given to highlight these features and capabilities.

1.6 VIZ.06: A Virtual Observatory for the Ionosphere, Thermosphere and Mesosphere Community – by Yee, Jeng-Hwa presented by Nylund, Stuart

Status of First Author: Nonstudent

Authors: Jeng-Hwa Yee, JHU/APL, sam.yee@jhuapl.edu; Robert McGuire, NASA/GSFC, robert.e.mcguire@nasa.gov; Elsayed Talaat, JHU/APL, elsayed.talaat@jhuapl.edu; Dieter Bilitza, NASA/GSFC, bilitza@ndads.gsfc.nasa.gov; Stuart Nylund, JHU/APL, stuart.nylund@jhuapl.edu
Abstract: The ionosphere, thermosphere and mesosphere (ITM) community studies an area of the atmosphere that is a transition region between the atmosphere and space, where many important physical and chemical processes change dramatically temporally and spatially. As a result, the areas of studies within the ITM community span a wide spectrum of scientific subjects in geophysics and space physics. The relevant data for the community collected during the past few decades consequently come from a variety of sources including ground and space-based instruments as well as from modeling and data assimilation. As the different sub-fields mature, a system-oriented approach to understand the ITM as a whole and its relationship to the sun and the surrounding geospace environment is critical. This approach requires a data system with efficient access to all data sets (present and historical) relevant to disciplines across agencies, including NASA, NSF, NOAA and others.
A preliminary Virtual ITM Observatory (VIO) concept for such a data system is presented as a grassroots level effort by the community which leverages current resources. The design incorporates a modular framework which accepts distributed data and services from across the community and encourages widespread participation. Data can be added as both new missions and historical holdings become available, and services added or replaced as technologies and standards evolve. The core VIO middleware is based upon a set of principles: centralized browse and query/retrieval of distributed resources, access to data reader software and other tools, and integration of current data with data from previous missions and long-term data sets. The VIO concept is presented to the community for discussion and community-wide input as part of a definition phase.

1.7 VIZ.07: CEDAR-RELATED DATA AND MODEL SERVICES AT THE SUN EARTH CONNECTION ACTIVE ARCHIVE (SECAA) – by Bilitza, Dieter

Status of First Author: Nonstudent

Authors: D. Bilitza (1), R. McGuire (2), N. Papitashvili (3), T. Kovalick (3), R. Candey (2), D. Han (2) (1) Raytheon ITSS, GSFC, Code 632, Greenbelt, MD 20771, USA, (2) SPDF, GSFC, Code 632, Greenbelt, MD 20771, USA (3) QSS, GSFC, Code 632, Greenbelt, MD 20771, USA, bilitza@mail630.gsfc.nasa.gov

Abstract: NASAs Sun Earth Connection active Archive (SECAA) provides access to a large volume of data and models that are of relevance to the Coupling, Energetics and Dynamics of Atmospheric Regions (CEDAR) program. SECAA has developed a number of web systems to facilitate user access to this important data source and is making these services available through Web Services (or Application Programming Interfaces, API) directly to applications such as VxOs. The Coordinated Data Analysis web (CDAWeb) lets user plot data using a wide range of parameter display options including mapped images and movies. Capabilities also include parameter listings and data downloads in CDF and ASCII format. CDAWeb includes data from most of NASA's currently operating space science spacecraft including ACE, Cluster, FAST, Genesis, Geotail, IMAGE, IMP-8, SAMPEX, SOHO, Ulysses, Wind and Polar. The most recent addition are data from the TIMED GUVI instrument. Intensities at all five GUVI spectral bands can be viewed as line plots, images and movies using various geographical projections. TIMED TIDI wind vector data will be available on CDAWeb shortly. SECAA maintains and supports the Common Data Format (CDF) including software to read and write CDF files. Most recently a translator services has been added for CDF translations to netCDF, FITS, CDFML (XML representation of CDF) and ASCII and netCDF-to-CDF, netCDF-to-ASCII, FITS-to-Cdf, and CDFXML-to-CDF SSCWeb provides the ability to plot orbits for the majority of space physics satellites (including TIMED, UARS, DMSP, NOAA, LANL etc.) and a query interface for magnetic field line conjunctions between multiple spacecraft and ground stations and for magnetic region occupancy. Recently an Interactive 3-D orbit viewer was added to SSCWeb. Access to legacy data from older ITM satellite missons is provided through the ATMOWeb system with the ability to generate line plots for user-selected time periods and plotting options and to download data subsets in ASCII format. Recently added capabilities include a scatter plot option and

linear regression fits for any pair of parameters. Optional upper and lower boundaries let users filter out specific segments of data and/or certain ranges of orbit parameters. We will also present the newest version of the web portal to SECAAs models catalog, ftp archive, and web interfaces. The web interfaces (Fortran, C, Java) let users compute, list, plot, and download model parameters for selected models (IRI, IGRF, MSIS CIRA, AE AP-8).

1.8 VIZ.08: The Living With a Star Scientific Resource Access System: A Concept for Getting the Information to Do Science – by Daley, Rose

Status of First Author: Nonstudent

Authors: Lis Immer (JHU/APL); Brand Fortner (JHU/APL); Michele Weiss (JHU/APL); Julia Jen (JHU/APL); Josh Steele (JHU/APL); Barry LaBonte (JHU/APL) **Abstract**: Answering complex science questions often means that a scientist must find and use a variety of scientific resources. These resources can include static data in various formats, complex data assimilation models, and conversion and analysis tools. Although the wide acceptance of the Internet has led to an explosion of accessible scientific resources, it has also created a Babel of incompatible formats, data descriptions, and access methods. At the Johns Hopkins University Applied Physics Laboratory, we have devised a concept that uses metadata and commonly understood scientific concepts to provide easier discovery and access to these necessarily heterogeneous resources for doing science. This concept simplifies the integration of resources in a single system, and enables the interconnection of complex data systems including virtual observatories. Frequently, adding resources to data systems requires the development of specialized software to identify and supply data. Our goal is to eliminate the need to create this specialized software and instead utilize existing protocols, formats, and metadata. We will present the status of our efforts to demonstrate this concept.

1.9 VIZ.09: A Prototype for a Virtual Solar-Terrestrial Observatory – by Fox, Peter presented by Emery, Barbara

Status of First Author: Nonstudent

Authors: Fox, P.A. (pfox@ucar.edu), Garcia, J.(jgarcia@ucar.edu), West, P. (HAO/NCAR) **Abstract**: The VSTO is proposed to be a scalable environment for searching, integrating, and analyzing databases distributed over the Internet. The VSTO would comprise a system of data, model, tool and material archives containing items from space- and ground-based instruments, individual and community modeling efforts, taken from NCAR, US universities and international sources, and from NSF- and NASA-funded groups. A key element of the VSTO is an integrated data-mining and analysis capability that can be applied both across and within databases. The capabilities of a VSTO are intended to be available to a wider community of scientists, educators, and the public and thus is intended to be a natural conduit for education and public outreach in solar solar-terrestrial and space physics. This presentation will outline the key functionality, proposed architecture and technologies that will be used in assembling the VSTO. We will also present past experience in building elements of data and collaborations system and the lessons learned.

2 Tuesday Evening 29 June 2004 Poster Session Abstracts, Polar and high-latitude aeronomy

2.1 POL.01: Seasonal and Kp Variations in the Auroral Electron and Ion Hemispheric Power after Intersatellite Adjustments – by Emery, Barbara

Status of First Author: Nonstudent

Authors: Barbara A. Emery (HAO/NCAR, emery@ucar.edu), David S. Evans (SEC/NOAA, david.s.evans@noaa.gov), Frederick J. Rich (AFRL, frederick.rich@hanscom.af.mil), Weibin Xu (HAO/NCAR, xuw@ucar.edu), Katharine Kadinsky-Cade (AFRL, katharine.kadinsky-cade@hanscom.af.mil), Ernest Holeman (Boston College, ernest.holeman@hanscom.af.mil) and M. Susan Greer (SEC/NOAA, sue.greer@noaa.gov)

Abstract: Twenty-six years of low energy auroral electron and total hemispheric power indices from 21 NOAA and DMSP satellites were combined to produce both hourly and daily median and average composite indices for the south and north hemispheres. The SEM-2 NOAA satellites also provided estimates of the auroral ion hemispheric power over the last 6 years. Daily median intersatellite correlations exceeded 70% most of the time after contamination or degradation issues were addressed, and the median daily values usually agreed within 5% overall after making baseline adjustments that ranged within a factor of two. Initial corrections were made to eliminate sunlight contamination, data dropouts over the auroral oval, the degradation of sensors over time, high spurious count rates, and increased noise at the end of a satellite lifetime. Adjustments were also made in most satellites such that the ratio of the south to north electron or total hemispheric power was approximately one over a year. Kp relations are given for both the electron and the ion hemispheric power. The ratio of the concurrent median daily hemispheric power from both hemispheres shows that the winter values are almost 30% higher than the summer values during solar maximum, and about 5% higher in solar minimum conditions. The winter/summer concurrent ratios of the ion hemispheric power are opposite to those of the electrons, showing increases in the concurrent summer to winter ratios of about 27% independent of solar cycle. The seasonal effects are also apparent in each Kp level since the summer ion contribution is about 75% larger than winter for Kp less than 1-, decreasing to about 20% larger for Kp greater than 2+. The ion hemispheric power from both low and medium energies is estimated to be 2 to 3 times larger than the estimates from ions less than 20 keV. Ions contribute most to the total hemispheric power, up to 30%, in quiet conditions, and contribute between 10-20% for Kp 2 or more.

2.2 POL.02: Comparison Of One Year Of DMSP F13 Cross-Track Ion Drift Velocities With Real-Time AMIE Results – by Bekerat, Hamed

Status of First Author: Student NOT in the poster competition PhD

Authors: Hamed A. Bekerat1 , Robert W. Schunk1 , and Ludger Scherliess 1
1 Center For Atmospheric And Space Sciences, Utah State University, Logan, UT84322
Aaron Ridley2 2 The University Of Michigan, 1411B Space Research Building Ann Arbor, MI 48109-2143

Abstract: The Assimilative Mapping Of Ionospheric Electrodynamics (AMIE) has been used in a wide range of studies pertaining to the magnetosphere, ionosphere and thermosphere. In these studies historical data from several different data sources have been assimilated. In its real-time mode (rt-AMIE), only data from an array of ground-based magnetometers are assimilated in real-time and convection patterns are produced in one-minute increments. However, the reliability of these real-time patterns for applications involving ionosphere-thermosphere specifications and forecast has never been systematically tested. To address this issue, a comparison of one year of DMSP F13 cross-track ion drift velocities with real-time AMIE results has been conducted. First, for each high latitude DMSP velocity observation, the corresponding AMIE value was calculated. Then, the measured and calculated cross-track ion drift velocities were compared and criteria were established to determine whether or not the AMIE patterns fit

the measurements adequately. The comparisons were done for one year (1998) of satellite crossings of the northern polar region. In this poster we present the results of this comparison.

2.3 POL.03: SuperDARN Radar Measurements of Ionospheric Heater-Induced Field-Aligned Irregularities – by Bhatt, Asti

Status of First Author: Student in the poster competition PhD

Authors: A. N. Bhatt, Cornell University, astibhatt@hotmail.com F. T. Berkey, Utah State University, ftb@cc.usu.edu C. M. Swenson, Utah State University, charles.swenson@usu.edu

Abstract: A series of ionospheric modification experiments were carried out in August 2003 and February 2004, to create artificial field-aligned irregularities (FAI) in the ionospheric F2 region using the high-power HF transmitter at HAARP heating facility, Gakona, AK. SuperDARN (Super Dual Auroral Radar Network) coherent scatter radar located at Kodiak Island, AK was used to scan the heated region over HAARP. It measured the power backscattered from the created irregularities. The primary purposes of these experiments were 1) to observe the dependence of this backscattered power from the FAI on the transmitter power from HAARP and 2) to observe the effects of ionospheric preconditioning on the backscattered power from the FAI. The results obtained from these power stepping experiments showed a nonlinear transmitter power dependence and ionospheric preconditioning effect on the backscattered power from the FAI. This document reports some of these results.

2.4 POL.04: Quantifying the Periodic Thermospheric Response for the April 14-24, 2002 Storm Period – by Curtis, Natalie

Status of First Author: Student in the poster competition Undergraduate

Authors: N. Curtis, Southwest Research Institute, ncurtis@swri.edu G.Crowley, Southwest Research Insitute, gcrowley@swri.edu C.Hackert, Southwest Research Institute, chackert@swri.edu J.Kozyra, University of Michigan, jukozyra@umich.edu R.G.Roble, HAO/NCAR roble@hao.ucar.edu

Abstract: The April 2002 storm was one of the largest at solar maximum. Its development was complex, and involved periodic inputs to the geospace system. We have simulated the storm using the NCAR TIMEGCM, with realistic high latitude inputs driven by measured Hemispheric Power and solar wind parameters.
The variability of the high latitude inputs has a significant effect on the thermospheric temperature, composition, density and wind responses, and the corresponding ionospheric electron density. In this paper, we examine the periodicity of the high latitude drivers, and the periodic response of the coupled thermosphere-ionosphere system. These results have important implications for operational space weather models, forecasting of the thermosphere-ionosphere state, and our understanding of measured variability.

2.5 POL.05: Insights from nonlocal theory on recent HF observations of high-latitude E region irregularities – by Drexler, Josef

Status of First Author: Student NOT in the poster competition PhD

Authors: Josef Drexler, U. of Western Ontario, Canada, jdrexler@uwo.ca J.-P. St.-Maurice, U. of Western Ontario, Canada, jstmauri@uwo.ca

Abstract: Milan et al. (Ann. Geophys., 22, 829, 2004) have recently reported on E-region backscatter from what appear to be very large aspect angles, with a Doppler shift that is consistent with the line-of-sight component of the ion drift velocity. We propose that the observed irregularities are the result of the nonlinear nonlocal evolution of decameter Farley-Buneman waves. We show how they arise not from high aspect angles as such, but rather from a strong gradient or discontinuity in their aspect angles, produced by a mode conversion due to the inhomogeneity of the medium. While their origin is not quite a

large aspect angle but rather a steeply changing one, these strongly damped modes truly represent, in fact, the eigenmode that one would expect at large aspect angles. That is to say: at large aspect angles, the two-stream expression that is often extrapolated from weakly growing or decaying modes is actually incorrect.

2.6 POL.06: Analysis of SuperDARN Electric Fields vs. Heppner-Maynard Electric Fields as a Driver for the Utah State University Time Dependent Ionospheric Model, with DMSP In Situ Data Comparisons – by Hogue, Chris presented by Groves, Clark

Status of First Author: Student NOT in the poster competition Masters

Authors: Hogue, Chris; AFIT; chris.hogue@afit.edu Groves, Clark; AFIT; clark.groves@afit.edu Sojka, Jan; USU; jjsojka@cass.usu.edu Ruohonemi, Michael; JHU/APL;

Abstract: Electric fields derived from the SuperDARN radar network are used to drive a simulation of plasma density structures in the high latitude ionosphere using the Utah State University Time Dependent Ionospheric Model for the study day of February 23, 2000. A side-by-side comparison is made with density structure output for a model run based on electric field inputs of Heppner-Maynard. DMSP data comparisons reveal a likely tongue of ionization in the polar cap during the study period which both model runs capture.

2.7 POL.07: Tracking of Polar Cap Ionospheric Patches – by Bust, Gary

Status of First Author: Nonstudent

Authors: Gary Bust Applied Research Laboratories, The University of Texas at Austin gbust@arlut.utexas.edu
Geoff Crowley Southwest Research Institute gcrowley@swri.edu

Abstract: Ionospheric patches are significant perturbations on F-region electron densities in the polar cap ionosphere. There are many questions related to their formation, transport, and eventual transformation into blobs on the nightside. The present study allows for a full three-dimensional convection analysis of the patch fate. Measurements provided by three high-latitude tomography arrays located in Greenland, Alaska and Scandinavia are supplemented by ISR, Ionosonde and DMSP measurements. The data are assimilated into a IDA3D a 3DVAR objective analysis algorithm. The background model for the analysis is the NCAR TIMEGCM, with comprehensive high latitude inputs. Results from this study demonstrate the cabability of tracking the 3D evolution of patches as they cross the polar cap.

2.8 POL.08: Modeling parameterization of anomalous resistivity in auroral return current region and application – by Lin, Tengfei

Status of First Author: Student in the poster competition Masters

Authors: Lin, Tengfei, Meers M. Oppenheim, Lars P. Dyrud Boston University (all three) ltf@bu.edu, meerso@bu.edu, ldyrud@bu.edu

Abstract: Intense electrical currents flow in and out of the Earth's high-latitude ionosphere creating the aurora borealis and other phenomena important to space scientists. Spacecrafts have shown that these regions of high current usually also support high voltages even though the predicted resistivity of the auroral ionospheric plasma is exceptionally small. A pending JGR paper, Electron hole resistivity in space plasmas by Dyrud et al., uses simulations to show that beam-driven currents, as expected to exist in the downward current region of the auroral ionosphere, will generate sufficient anomalous resistivity to explain the measured potential drops. These occur in simulations with a cold beam current going through warm plasma background. In our current work, we present resistivity measurements from simulations for a broad

range of input parameters appropriate for the auroral ionosphere. This parameterization shows that resistivity increases linearly with inverse beam temperature, exponentially with beam density, and almost linearly with beam velocity. It can vary by a factor of three with different velocities, a factor of ten with different temperatures and a factor of three order magnitude with density from 0.35 to 0.8 total electron density. A simple functional relationship seems to summarize all these features. We apply all these results to the 3000 km space, successfully accounting for the measurements with two tests on the theory.

2.9 POL.09: Mesospheric and thermospheric neutral wind results from a newly installed multi-emission Fabry Perot interferometer in Resolute Canada – by Wu, Qian

Status of First Author: Nonstudent

Authors: Q. Wu NCAR/HAO qwu@ucar.edu S. C. Solomon NCAR/HAO stans@ucar.edu R. D. Gablehouse NCAR/HAO rdg@ucar.edu T. L. Killeen NCAR/HAO killeen@ucar.edu

Abstract: To study high latitude tides, upper thermosphere neutral winds and their responses to the ionosphere and magnetosphere coupling, and to support the future AMISR project, a new highly sensitive multi-emission Fabry Perot interferometer was installed in Resolute (75N) late last year. The instrument is capable of measuring neutral winds using three emissions: OH (87 km), O(1S) 557.7 nm (97 km), and O(1D) 630. nm (250 km). High accuracies of the neutral wind measurements allow more detailed studies of the high latitude tides in the MLT region. High latitude upper thermospheric neutral winds are valuable to the understanding of the ionosphere and magnetosphere interaction and the ion-neutral coupling. Accurate neutral wind measurements can help determine how much energy converted to neutral kinetic energy and how much lost to the joule heating. We see many collaboration opportunities with the future AMISR in the study of high latitude thermospheric dynamics and energetics, given that AMISR can provide ion drift, ion and electron densities, electron, ion, and neutral temperature profile while the FPI monitors the neutral winds at multiple levels. In this report, we will show neutral winds from this instrument and tidal analysis results based the neutral wind measurements.

2.10 POL.10: TDIM Model Studies for the October-November 2002 HLPS Campaign – by Sojka, Jan

Status of First Author: Nonstudent

Authors: J. J. Sojka, CASS, Utah State University, sojka@gaim.cass.usu.edu
L. Zhu, CASS, Utah State University, zhu@cc.usu.edu
M. David, CASS, Utah State University, michael@sim2.cass.usu.edu
R. W. Schunk, CASS, Utah State University, schunk@cc.usu.edu

Abstract: The 3 October through 4 November 2002 HLPS campaign is unique in that the Svalbard EISCAT ISR was operating continually. SuperDARN observations provide global scale patterns of convection required by the TDIM ionospheric model to simulate this period. Results of these simulations will be presented as plasma parameters at the DMSP altitude of 840 km as the satellites pass over the Svalbard location twice per day. These simulated results are also presented for comparison with the DMSP observations to be presented by Hairston et al.

2.11 POL.11: Validating the UAF EPPIM vs Ionosonde Readings – by McAllister, Jeff

Status of First Author: Nonstudent

Authors: McAllister, Jeff (mcallist@arsc.edu) and Maurits, Sergei (maurits@arsc.edu) – Arctic Region Supercomputing Center **Abstract**: The UAF EPPIM is a 3D time-dependent model of the northern polar ionosphere. It is based on first-principles chemistry and dynamics with a minimum of statistical

generalizations. It can be run in batch/postanalysis mode using stored inputs or in real time providing forecasts of ionospheric conditions. This poster shows model comparisons with foF2 readings (the highest frequency which will reflect instead of passing through the F2 layer) with ionosonde readings at Qaanaq (76 N), Sondrestrom (67 N), King Salmon (59 N), and Goose Bay (53 N) for the representative periods of December 2003, March 2004, and May 2004. More validations are available at http://www.arsc.edu/SpaceWeather.

2.12 POL.12: F-region Ion Temperature Distributions over the Polar Cap and the Auroral Region – by Maeda, Sawako

Status of First Author: Nonstudent

Authors: Sawako Maeda (Kyoto Womens University, smaeda@kyoto-wu.ac.jp) Satonori Nozawa (STEL, Nagoya University, nozawa@stelab.nagoya-u.ac.jp) Yasunobu Ogawa (STEL, Nagoya University, yogawa@stelab.nagoya-u.ac.jp) Asgeir Brekke (The Auroral observatory, University of Tromsoe, asgeir@windows.phys.uit.no) Shin-ichiro Oyama (Geophysical Institute, University of Alaska Fairbanks, soyama@gi.alaska.edu)

Abstract: Simultaneous measurement of the ion temperature by the EISCAT UHF radar at Tromsoe(UHF radar, 69.6 N) and the EISCAT Svalbard radar at Longyearbyen (ESR, 78.2 N) was performed in a special program experiment between 10:00 UT in July 09 and 13:00 UT in July 10, 2001. The purpose of this study is to investigate the effect of the frictional heating on the ion temperature along the low-latitude boundary of the polar cap and the auroral zone. Previous study by using the CP-2 data of the UHF radar and the ESR showed that the E-region ion and neutral temperatures at Longyearbyen were higher than those at Tromsoe during the daytime (Maeda et al., 2002). In order to investigate temperature distributions over the meridional distance of about 1000km in further detail, a 27 hours special program experiment with the UHF radar and the ESR was carried out by using the north and south beams with the low elevation angle of 30 degree combined with the cp2-type beams. In the CP-2 mode the line of sight of the combined transmitter and receiver antenna in Tromsoe are pointed into four consecutive positions with a dwell time of approximately one minute in each position, leaving the full cycle time of the antenna to be six minutes. The horizontal distance among 11 scattering volumes ranges between about 50 km and 1400 km at the altitude of 250 km. The cycle time of the EISCAT UHF radar and the ESR was 45 minutes. The antenna cycles of the two radars are as follows: EISCAT UHF radar; north to CP2 to south to CP2 ESR; south + FA to CP2L to south + FA to CP2L. The temperatures measured by the beams with various aspect angles were converted to be the field-aligned temperature taking into account the anisotropy when they were compared with each other.
The main results are as follows. The ion temperature at 280 km height went up to be 1500 K above the Tromsoe site for a few hours after the local midnight on July 10. The increase of the ion temperature was observed with the north beam of the UHF radar from 02MLT to 06MLT. The high temperature region appeared at south beam of the ESR from 06 MLT to 09MLT. At 12 MLT, the ion temperature above the ESR site was highest among the others.
From an inspection of the magnetic field variations measured by the IMAGE ground-based magnetometers, it was suggested that the high temperature region after the local midnight corresponded to the region of the strong westward auroral jet current, and the high temperature region in the morning sector was coincident with the polar cap boundary. It was found that the dayside ion temperature was high in the polar cap of high-speed antisunward flow from the DMSP plasma drift data.
References: Maeda et al., Ann. Geophys., 20, 1415, 2002.

2.13 POL.13: Observations of Neutral Wind Gradients in the Auroral Oval During Two Substorm Events – by Zhan, Tianyu presented by Larsen, Miguel

Status of First Author: Student NOT in the poster competition Masters

Authors: Tianyu Zhan, Clemson Univ. tzhan@clemson.edu; Miguel F. Larsen, Clemson Univ. mlarsen@clemson.edu **Abstract**: The CODA and JOULE sounding rocket experiments were carried out at Poker Flat Research Range on February 21, 2002, and March 27, 2003, respectively. The CODA and JOULE launches were both characterized by significant gradients in the plasma drifts, and thus the forcing, although CODA occurred during a substorm that followed a long period of quiet conditions while the JOULE experiment occurred after many hours of active conditions. Three chemical tracer rockets in CODA and one in JOULE were launched successfully as part of the experiments. The trimethyl aluminum (TMA) trails released on the upleg and downleg portion of the flight between approximately 80 and 180 km altitude thus provided measurements of the horizontal gradients in the neutral flow as a function of altitude under different conditions. The poster focuses on the wind measurements that were obtained by triangulation of the trail images from three sites and the comparison of the profiles under quite and disturbed condition. Typical accuracies are 5-10 m s-1 over the altitude range covered by the releases.

2.14 POL.14: Comparison of ionospheric tomographic data with the UAF theoretical polar ionospheric model – by Kulchitsky, Anton

Status of First Author: Nonstudent

Authors: Anton Kulchitsky (Geophysical Institute, University of Alaska, Fairbanks, anton@kulchitsky.org); Brenton Watkins (Geophysical Institute, University of Alaska, Fairbanks, bjw4072@mailblocks.com); Sergei Maurits (Arctic Region Supercomputing Center, University of Alaska, Fairbanks, maurits@arsc.edu); Ed Fremouw (NorthWest Research Asociates, Inc., ed@nwra.com).

Abstract: The UAF theoretical polar ionospheric model (UAF EPPIM) computes 3D equations of mass, momentum, and energy balance for the ion species in the ionosphere to determine ion and electron parameters in the polar ionosphere region using a parallel numerical code on an Eulerian grid. To validate the model output we used ionospheric electron density tomography data slices from the Alaska region along Cordova, Big Delta, Fort Yukon and Kaktovik direction (close to the 145-deg west geographic meridian). The tomographic data are gathered on a routine basis at the Alaska HAARP facility (see details on-line at http://www.haarp.alaska.edu). The tomography results are compared with the corresponding 2-D cross-sections of the UAF EPPIM outputs. Data comparisons are performed during one particular day (May 1, 2003) and for different days during 2003 for particular local times. Large-scale data comparisons show a rather good quantitative and qualitative coincidence of the experimental data and the model results. An on-line real-time version of the UAF EPPIM, and model validation data, are available at http://www.arsc.edu/SpaceWhether or http://ion.gi.alaska.edu.

2.15 POL.15: DMSP Data for the October-November 2002 HLPS Campaign – by Hairston, Marc

Status of First Author: Nonstudent

Authors: Marc Hairston, W. Robin Coley, Kelly Ann Drake, and Rod Heelis Center for Space Sciences University of Texas at Dallas

Abstract: During the 3 October 4 November 2002 HLPS campaign period there were two operational DMSP spacecraft: F13 in a dawn-dusk polar orbit and F15 in a 0930-2130 LT polar orbit. Each of these spacecraft passes over the Svalbard radar location (20 00 E and 78 00 N) twice a day, thus providing four samples a day of the ionospheric conditions at that location. DMSP provides data about the velocity, temperature, density, and composition of the thermal plasma at 840 km. We will present the daily DMSP data over the HLPS campaign from these four sample times. This dataset will provide an observational basis for the researchers modeling the ionosphere during this campaign.

3 Tuesday Evening 29 June 2004 Poster Session Abstracts, Mid-latitude thermosphere and ionosphere

3.1 MID.01: Ionospheric model based on Saint Santin incoherent scatter radar data – by Zalucha, Angela

Status of First Author: Student in the poster competition Undergraduate

Authors: Angela M. Zalucha, MIT Haystack Observatory, zalucha@uiuc.edu,
John M. Holt, MIT Haystack Observatory, jmh@haystack.mit.edu,
Shun-rong Zhang, MIT Haystack Observatory, shunrong@haystack.mit.edu

Abstract: Recently, a statistical model of ionospheric electron density, ion temperature, and electron temperature was made using Millstone Hill incoherent scatter radar data. Using the bin-fit technique developed for this model, a similar model has been constructed using Saint Santin incoherent scatter radar data from the years 1966 through 1987. The Saint Santin model generates local ionospheric variations with local time, day number, altitude (between 100-550 km), and the previous day's F107 index. The model is capable of reproducing major ionospheric phenomena seen in previous studies, as well as suggesting new features. A comparison between the Millstone Hill and Saint Santin models is also made.

3.2 MID.02: A turbulence case simulation of the Perkins instability in the TEC inhomogeneous condition – by Zhou, Qina

Status of First Author: Student in the poster competition PhD

Authors: Qina Zhou, John D. Mathews, Qiang Du, Penn State Univ, University Park. Clark A. Miller Univ. of Wisconsin-Madison

Abstract: With the high-accuracy spectral method code we have developed, a turbulence (spread-F) case in the TEC (Total Electron Content) horizontally inhomogeneous initial condition is simulated on a spatial scale of 256 times 256 km2 and a Gaussian initial TEC/conductivity distribution. This simulation is motivated by the frequently occuring horizontal TEC gradients over Arecibo [Zhou, 2000; Zhou et al., 2004]. The simulation results display strong nonlinear behavior with the system gradually moving into a turbulence outcome. Fractal-like structures that develop in the simulation are similar to ionospheric structure seen in incoherent scatter radar observations and in all-sky camera images [Mathews et al., 2001; Garcia et al., 2000]. It seems that the ExB instability finally involves in the process.

3.3 MID.03: Comparison of IRI-2001 with TOPEX TEC measurements – by Jee, Geonhwa

Status of First Author: Student in the poster competition PhD

Authors: Geonhwa Jee, Robert W. Schunk and Ludger Scherliess, Center for Atmospheric and Space Sciences, Utah State University jee@cc.usu.edu **Abstract**: During the last decade, the OPEX/Poseidon mission has provided a wealth of data pertaining to Total Electron Content (TEC) measurements over the oceans, where conventional measurements are sparse. In this study, a comprehensive comparison of the TOPEX TEC measurements with the recent version of the International Reference Ionosphere (IRI-2001) was performed. The study covered solar cycle, seasonal, geomagnetic activity, and longitudinal variations. The resulting comparisons can be utilized to improve the IRI. First, it was found that both the IRI and TOPEX TEC show a negligibly small geomagnetic dependency, regardless of solar activities and seasonal conditions. For solar activity, however, not only the TECs from the IRI and TOPEX measurements, but also the difference between them strongly depend on the solar activities. The comparison also shows that the daytime low-latitude ionosphere from the IRI develops always earlier than the corresponding TOPEX measurements, appearing as the overestimates of IRI TEC at around 7 MLT in the morning. With respect to the annual and seasonal variations of TEC, the TOPEX TEC shows stronger annual and semiannual

anomalies than the IRI TEC both at low latitudes and at upper mid-latitudes. However, both the IRI and TOPEX TECs show similar seasonal anomaly only for high solar activity. Finally, the longitudinal variations of the IRI TEC shows good agreement with the TOPEX measurements for low solar activity, but for high solar activity, quite large discrepancies occur in the Pacific sector.

3.4 MID.04: Photochemical Modeling of E-layer Variability – by Moore, Luke

Status of First Author: Student in the poster competition PhD

Authors: Luke Moore, Tengfei Lin, Michael Mendillo, Carlos Martinis, Boston University, Center for Space Physics, moore@bu.edu, ltf@bu.edu, mendillo@bu.edu, martinis@bu-ast.bu.edu **Abstract**: Using a time-dependent one-dimensional photochemical model, we reproduce observed diurnal behavior of the E-layer. The SOLAR2000 model is used for the Sun's irradiance, the MSIS model for a neutral atmosphere that varies day-to-day, and data from the SNOE satellite for NO densities. We separate and explore the E-layer effects of (a) night time ionization, (b) secondary ionization, and (c) different NO density parameterizations. Finally, we extract the sources of variability in the E-layer, and find that the dominant source is solar flux variability.

3.5 MID.05: Seasonal and Longitudinal variations of Mid-latitude Spread F based on ISS-b observation. – by Mwene, Anthony

Status of First Author: Student NOT in the poster competition PhD

Authors: Mwene, Anthony W. B. H. Center for Space Sciences, Univ. of Texas at Dallas tonymusumba@hotmail.com G. D. Earle, W. B. H. Center for Space Sciences, Univ. of Texas at Dallas, earle@utdallas.edu

Abstract: A preliminary study of the global distribution of spread echoes fron the Japanese Ionopsphere Sounding Satellite(ISS)-b using the topside sounding data has been undertaken.Significant longitudinal and seasonal variations in the Equatorial Spread Echoes are observed.To validate our approach we compare Low-latitude sounder data to well known seasonal variations in scintillation indices at specific longitudes.After establishing the validity of the approach, we study the occurence probabilities for Mid-latitude Spread F as a function of geographic location over the interval from August 1978 to November 1980.

3.6 MID.06: Relative concentrations of molecular and metallic ions in midlatitude intermediate and sporadic-E layers – by Roddy, P

Status of First Author: Student in the poster competition PhD

Authors: P. A. Roddy, W. B. H. Center for Space Sciences, Univ. of Texas at Dallas, roddy@utdallas.edu G. D. Earle, W. B. H. Center for Space Sciences, Univ. of Texas at Dallas, earle@utdallas.edu C. Swenson, Utah State Univ. C. G. Carlson, Utah State Univ. T. W. Bullett, Air Force Res. Labs.

Abstract: A NASA sounding rocket launched from Wallops Island, VA (37.84 N, 75.48 W) on June 29, 2003 at 1:50 LT made the first in-situ measurement of the relative concentrations of Fe+, Mg+, O2+, and NO+ within a low altitude intermediate layer. Ion composition measurements were made throughout the flight and included observations of three separate regions having high concentrations of metallic ions: the intermediate layer, the sporadic-E layer, and a third layer above 160 km altitude. These observations demonstrate that metallic ions may play a significant role in the dynamics of the nighttime E and F region ionosphere at midlatitudes.

3.7 MID.07: Ionospheric Models Based on ISR Observations at Millstone Hill, St. Santin and Shigaraki – by Zhang, Shunrong

Status of First Author: Nonstudent

Authors: Shun-Rong Zhang(1), John M. Holt(1), William C. Rideout(1) Angela M. Zalucha(1,2), Christine Amory-Mazaudier(3), Seiji Kawamura(4), and Shoichiro Fukao(5)
(1)MIT Haystack Observatory (2)UIUC Department of Physics (3)CETP / CNRS, France (4)National Institute of Information and Communications Technology, Applied Research and Standards Department, Japan (5)Kyoto University, Research Institute of Substainable Humanosphere, Japan

Abstract: Ionospheric data from incoherent scatter observations are being accumulated for 1-3 solar cycles over the world. Most of these data have been assemblied into the Madrigal system (http://www.openmadrigal.org) hosted at Millstone Hill and most other ISR sites as well. By making use of such a valuable data source, we have been able to construct empirical ionospheric models for several incoherent radar sites, including electron density and plasma temperatures models over Millstone Hill (locally and regionally) in Northern America, St Santin in Europe, and Shigaraki in Eastern Asia, as well as a revised high latitude convection model derived from Millstone Hill radar's wide coverage experiments. These models are Web based user-friendly, and provide rela-time estimate of ionosphere conditions using near real-time solar-geophysical indices and the IMF data (http://www.haystack.mit.edu/madrigal/Models/). Models for other ISR sites are under development. These space weather models and the large ISR data source make feasible further studies of ionospheric climatology, variabiloty, and long-term changes.

3.8 MID.08: Variability of terrestrial E layer: modeling NmE – by Lin, Tengfei

Status of First Author: Student in the poster competition Masters

Authors: Tengfei Lin Center for space physics, Boston University ltf@bu.edu

Abstract: The star creates ionospheres across our solar system. [Tobiska, et al., 2000] provides empirical solar irradiance data, and [Hedin, A. E., 1991] provides neutral atmosphere data of the earth, both required for Chapman theory of studying ionosphere structures. Applying only 3 EUV and 3 UV bands out of all 39 bands of irradiance data creates NmE magnitude, position, day-to-day variability of 19 days studied, NmE2 E10.7 index linear slope matching the measurement perfectly, implying that terrestrial E layer is not only position characterized, but also band characterized. This model also hypothesizes that electron recombination rate is always equal to electron ionization rate, which implies that electron density is always irradiance controlled, and has nothing to do with its previous status. This is proved by the measurement. The morning section of NmE is quite similar to the afternoon section, but one follows night conditions and one follows noon conditions. The model implies that NmE2 E10.7 index slope is independent of local time and station chosen. Because 19 days is a relatively short period, so the day dependence is not tested. However, its independence through the year is suggested.

3.9 MID.09: A Two-Year Summary of Field-Aligned Irregularity Observations at Sub-Auroral Latitude – by Meyer, Melissa

Status of First Author: Student in the poster competition PhD

Authors: Melissa Meyer, University of Washington, mgmeyer at ee.washington.edu
and
John Sahr, University of Washington, jdsahr at ee.washington.edu

Abstract: We present a statistical summary of the Doppler features extracted from over 21,000 independent E-region irregularity observations made during 2002 and 2003 with the Manastash Ridge Radar, a unique, high-resolution instrument which passively detects the scatter of commercial FM radio broadcasts near 100 MHz. The radar field of view is in the sub-auroral zone (southwestern Canada); we

discuss possible origins of wave instabilities that may lead to coherent backscatter from this region. We compare our results with other VHF coherent scatter data from both high- and mid-latitudes, and find a strong dependence on irregularity scale-length (transmitter frequency) and geomagnetic latitude for secondary wave turbulence. We also show trends in our data with respect to local time and geomagnetic activity (as measured by the Kp index). Finally, we are able to operate the radar continuously due to the uninterrupted illumination of commercial transmitters; this allows us to also determine the annual variation of the irregularities we observe.

3.10 MID.10: The Sporadic E Layer Instability in the Nighttime Midlatitude Ionosphere – by Cosgrove, Russell

Status of First Author: Nonstudent

Authors: Russell B. Cosgrove SRI International Roland T. Tsunoda SRI International

Abstract: The wind shear theory for the formation of sporadic E (Es) layers has been around for over forty years. However, certain features of Es layers have defied interpretation, such as their tendency to organize into frontal structures with a peculiar northwest to southeast frontal alignment, and the phenomenon of quasi-periodic (QP) radar echoes. The latter are coherent radar echoes with broad Doppler spreads, suggesting large electric fields. The anomalous observations suggest a role for electrodynamics in Es layers that has hitherto gone undescribed. Below, we describe our finding that the configuration of an Es layer at a wind shear node is in fact unstable at night, due to electrodynamical forces driven by the same wind shear responsible for the original layer formation. The instability is similar to the F layer Perkins instability, in that the growing modes are plane-wave-shaped altitude modulations of the layer, but has a growth rate nearly two orders of magnitude larger. The growth rate maximizes for modes with phase fronts aligned northwest to southeast, which would seem to explain the above mentioned observations of frontal structures. The growth phase involves strong polarization electric fields, which may provide an explanation for QP echoes. In recent work we have found that the Es layer instability couples to the Perkins instability, by way of electric fields mapping between the E and F regions, and can thereby increase the growth rate of the F region instability by up to five times.

3.11 MID.11: Coupling of the Perkins Instability and the Sporadic E layer Instability – by Cosgrove, Russell

Status of First Author: Nonstudent

Authors: Russell B. Cosgrove SRI International Roland T. Tsunoda SRI International

Abstract: Tsunoda and Cosgrove [2001] recently pointed out that the F layer and sporadic E (Es) layers in the nighttime midlatitude ionosphere must be considered electrodynamically as a coupled system in light of the presence of a Hall polarization process in Es layers [Haldoupis et al., 1996; Tsunoda, 1998; Cosgrove and Tsunoda, 2001; 2002a] and the fact that kilometer-scale electric fields map efficiently between the E and F regions. They further noted the apparent presence of positive feedback between processes in those regions. Cosgrove and Tsunoda [2002b, 2003] have since shown that Es layers are unstable with properties not unlike those of the Perkins instability in the F region [Perkins, 1973], motivating the idea that the two instabilities may couple. Finally, Cosgrove and Tsunoda [2004] derived the linear growth rate for the coupled system of a Es layer and the F layer, thus realizing a unified formalism for the Perkins and Es layer instabilities. They found that the growth rate was significantly enhanced by the coupling. However, the growth rate computed in Cosgrove and Tsunoda [2004] was expressed only as the largest eigenvalue of a complex 3 by 3 matrix. Below we present a physical interpretation of the E-F coupled-layer instability using schematic diagrams. We present a circuit model for the coupled-layer system that provides a physical interpretation for the wavelength dependance of electric field mapping between layers, and allows quantitative predictions. Using the circuit model we derive a rule of thumb for computing the two growth rates of the coupled system from the isolated Perkins and Es layer instability growth rates. We compare the result with the exact computation of Cosgrove and Tsunoda [2004].

4 Tuesday Evening 29 June 2004 Poster Session Abstracts, Instruments and techniques for thermosphere and ionosphere observations

4.1 IAT.01: Multi-resolution (wavelet) based non-stationary covariance modeling for POLAR UVI data – by Matsuo, Tomoko

Status of First Author: Nonstudent

Authors: Tomoko Matsuo and Douglas W. Nychka, Geophysical Statistics Project/ National Center for Atmospheric Research
Dirk Lummerzheim, Geophysical Institute/ University of Alaska
tmatsuo@ucar.edu nychka@ucar.edu lumm@gi.alaska.edu

Abstract: The Ultraviolet Imager (UVI) on board the POLAR satellite provides us with an estimate of the auroral electron precipitation, in terms of characteristic energy and total energy flux, with excellent spatial coverage and high temporal resolution. These parameters are used to determine the enhanced conductivity due to ionization of the neutral atmosphere by aurora particles. Applying a systematic statistical analysis to this data set, the spatial and temporal coherence of the auroral conductivity can be quantified. Such quantification is valuable not only for modeling of the background error covariance, which is required in data assimilation procedures for high-latitude ionosphere such as Assimilative Mapping of Ionospheric Electrodynamics (AMIE) procedure of Richmond and Kamide [1988], but also for understanding of physical mechanisms of the aurora at the stage of the field lacking a good physical model. Nychka et al. [2002] demonstrated that wavelets (multi-resolution basis) can provide versatile methods for introducing non-stationary spatial structure at various spatial scales. This idea is used to represent the spatial structure and stochastic features of the auroral electron precipitation: a process that is highly non-stationary, inhomogeneous, and anisotropic.

4.2 IAT.02: A New Approach to the Analysis of the Arecibo World Day Data – by Nikoukar, Romina

Status of First Author: Student in the poster competition PhD

Authors: Romina Nikoukar-UIUC-nikoukar@uiuc.edu Farzad Kamalabadi-UIUC-farzadk@uiuc.edu Michael sulzer-NAIC-msulzer@naic.edu Erhan Kudeki-UIUC-erhan@uiuc.edu Sixto Gonzalez-NAIC-sgonzalez@naic.edu

Abstract: Accurate and efficient extraction of altitude profiles of ionospheric parameters from incoherent scatter radar (ISR) measurements remains challenging due to two major issues: Range smearing of the information from one altitude over a range of altitudes is the first problem which is a non-ideal effect introduced into the radar data by the finite length of the transmitted pulse. The second complication is caused by the highly nonlinear relationship between the ISR spectrum and the ionospheric parameters. The conventional method, currently used at Arecibo, fits the parameters at coarsely spaced individual altitudes. Hence, achieving a satisfactory spatial resolution is the limitation of this method.
In order to improve the spatial resolution, we propose a technique in which the ionospheric ACF, and not the parameters themselves, are extracted at finely-spaced altitudes. This is accomplished by performing a set of 1-D deconvolutions for each time lag on the measured data ACF. Regularization techniques are exploited to overcome the numerical instabilities due to the ill-conditioned nature of the deconvolution problem. Once the ionospheric ACF at each altitude is obtained, there are several options to extract the altitude profiles of the parameters. One can perform the nonlinear least squares fitting at each range individually, or may include altitude models, such as polynomials, for the profiles over a few ranges.
The proposed new technique was examined on the New Arecibo World Day Data, where a pair of amplitude modulated pulses was exploited in transmission. The results of the new technique show superior performance over the conventional methods currently used in Arecibo regarding computational complexity and accuracy.

4.3 IAT.03: Topographic imaging using airglow and TEC – by Nicolls, Michael

Status of First Author: Student in the poster competition PhD

Authors: Michael J. Nicolls (Cornell University, mjn25@cornell.edu), Jonathan J. Makela (NRL, jmakela@ssd5.nrl.navy.mil), Drew Turner (Arecibo Observatory, dturner@naic.edu), Nestor Aponte (Arecibo Observatory, naponte@naic.edu), Michael C. Kelley (Cornell University, mikek@ece.cornell.edu), and Sixto A. Gonzalez (Arecibo Observatory, sixto@naic.edu)

Abstract: The intensity of the most commonly observed F-region airglow emission, that of O(1D) at 630.0-nm, is a function of the ionospheric height and the ionospheric density. These parameters in general are related in a complex fashion to the intensity of the emission. Here we discuss the problem of deriving ionospheric parameters from the emission intensity. We present a technique using total electron content (TEC) from GPS combined with the 630.0-nm intensity to estimate hmF2 and NmF2. We also discuss the method of using multiple wavelength filters (specifically, the 777.4-nm emission produced by radiative recombination of O+) to estimate the ionospheric parameters. Using the 630.0-nm intensity and either TEC or the 777.4-nm intensity, it is possible to produce good estimates of hmF2 and NmF2 by making some assumptions about the ionosphere. However, when all three are measured simultaneously, hmF2 and NmF2 can be deduced nearly unambiguously. Ionospheric topography maps can be created, giving hmF2 and NmF2 over a very wide area (1000 km by 1000 km). This result demonstrates the potential benefits for the colocation of imagers and dual-frequency GPS receivers. With the recent acquisition of an all-sky imager and a dual-frequency GPS receiver at the Arecibo Observatory, it is our intention to produce such maps in near real-time.

4.4 IAT.04: Frequency and Damping Factor Estimation for Meteor Radar Signals – by Kang, Chunmei

Status of First Author: Student NOT in the poster competition PhD

Authors: Chunmei Kang, Department of Aerospace Engineering Sciences, University of Colorado, chunmei.kang@colorado.edu Scott Palo, Department of Aerospace Engineering Sciences, University of Colorado, scott.palo@colorado.edu

Abstract: In this paper we analyze the factors which affect the estimation precision of the frequency and damping coefficient for the meteor radar signals. The Fast Maximum Likelihood (FML) algorithm is chosen as the signal estimation scheme. The likelihood function is sharper for low damping factors while flatter for high damping factors, thus adding to the difficulty in detecting highly damped signals. Damping factor estimation can be categorized in three stages: (1) For low SNR the value of the damping coefficient is underestimated. (2) For high SNR and large damping values the damping coefficient is overestimated. (3) For high SNR and low damping coefficients the estimate converges to the true value. These results indicate that the determination of damping coefficients from meteor radar signals is sensitive to SNR and the damping coefficients themselves. These biases may affect geophysical inferences such as diffusion and temperature determined from meteor radar signals. For comparison, global maximum search of likelihood function is also investigated. It gives higher estimation precision and lower estimation variation for low SNR, however at the cost of large computation.

4.5 IAT.05: Toward Determining the Effective Volume for Potential Backscatter in Coherent Radar Studies of the Ionosphere – by Meyer, Melissa

Status of First Author: Student NOT in the poster competition PhD

Authors: Melissa Meyer, University of Washington, mgmeyer at ee.washington.edu
John Sahr, University of Washington, jdsahr at ee.washington.edu

Abstract: Through consideration of the aspect angle criterion for field-aligned irregularities and radar observing geometry, we determine the range dependence of the potential scattering volume for coherent backscatter measured by the Manastash Ridge Radar. We intend to generalize this procedure into a model that can be applied to any radar observing from an arbitrary location. This model will be useful in determining the potential severity of clutter imposed on RF remote sensing systems due to ionospheric turbulence (or, in the case of an auroral radar, the likelihood of observing irregularity scatter at a given range). We also demonstrate a high-resolution experimental technique for validating the theoretical upper altitude bound for two-stream wave instability and growth.

4.6 IAT.06: Initial Results of a New IS Mode at Jicamarca – by Rodrigues, Fabiano

Status of First Author: Student in the poster competition PhD

Authors: F. S. Rodrigues and D. L. Hysell Cornell University, USA
J. L. Chau Radio Observatorio de Jicamarca, Peru

Abstract: This poster presents initial results of a new Incoherent Scatter (IS) mode for Jicamarca radar that combines the Double Pulse mode and the Long Pulse mode. Results include height profiles of plasma density, electron and ion temperatures, and ion composition from 150 km up to 1600 km. This operation mode will provide data support to C/NOFS (Communication/Navigation Outage Forecasting System) and DMSP (Defense Meteorological Satellites Program) satellites.

4.7 IAT.07: A new method for separating seasonal and tidal variations from space-based measurements: Application to TIMED/SABER temperature measurements – by Zhang, Xiaoli

Status of First Author: Student NOT in the poster competition PhD

Authors: Xiaoli Zhang, University of Colorado at Boulder, xiaoli.zhang@colorado.edu Jeffrey M. Forbes, University of Colorado at Boulder, forbes@colorado.edu Scott E. Palo, University of Colorado at Boulder, scott.palo@colorado.edu

Abstract: Satellite missions like UARS and TIMED have high-inclination, slowly precessing low-earth orbits. Because of the quasi-Sun-synchronous feature, the instrument, i.e. SABER on the TIMED mission, can make measurements each day within only two very narrow local time bins either on upleg or downleg. There local time bins slowly shift as the mission progresses, a yaw perid is required to complete a 24 hour local time cycle. The yaw period of SABER is either 60 days or 120 days depending on whether the latitudinal asymmetry is considered. So, seasonal variations of both background and tides naturally alias into tidal variation. We introduce a new method here to separate the seasonal background variation from the yaw period mean tidal variation. We apply this method to TIMED/SABER temperature measurements and present the results with scientific interpretations.

4.8 IAT.08: The Spatial Heterodyne Spectrometer: A New Tool for Atmospheric Science – by Watchorn, Steven

Status of First Author: Nonstudent

Authors: Dr. Steven Watchorn, Scientific Solutions, Inc., North Chelmsford, MA
email: steve@sci-sol.com

Abstract: This poster describes the Spatial Heterodyne Spectrometer (SHS), as a way to introduce it to a significant branch of atmospheric remote sensing. The SHS is a novel Fourier transform spectrometer, which provides outstanding interferometric performance over a broad range of wavelengths without scanning. Like conventional interferometers (Michelson, Fabry-Perot), it is more compact with higher

etendue at a given resolving power than grating spectrometers. However, being unscanned, it can be built far more robust than conventional interferometers, with relaxed flatness tolerances on critical optics. The robustness advantage is magnified by the advent of the monolithic SHS, in which all the critical optics are built into a single block.
Moreover, unlike Michelsons, the SHS can be adjusted from one observation to the next so that the center of its transformed spectrum always falls near the spectral lines of interest. A single SHS may thus produce easy-to-sample fringes in many wavelength regions. And, with a few other minor adjustments, one tabletop SHS can observe a emissions in a broad range of wavelengths far more efficiently than a single Fabry-Perot system.

4.9 IAT.09: Simulation of HF propagation in the ionospheric irregularities – by Wang, Lan

Status of First Author: Student NOT in the poster competition PhD

Authors: Lan Wang, University of Western Ontario,lwang28@uwo.ca John W. MacDougall, University of Western Ontario, jmacdoug@uwo.ca

Abstract: The Enhanced Polar Outflow Probe (e-POP) payload will be launched on a small satellite in a few years for exploring plasma and atmospheric outflow process in the polar region. This paper investigates the propagation of high frequency (HF) radio waves from a Canadian Advanced Digital Ionosonde (CADI) to the e-POP using ray-tracing simulation. Irregular structure in the ionosphere has a considerable effect on the characteristics of HF signals in that irregular enhancements or troughs lead to a complex propagation pattern and alter the signal amplitude, propagation time and direction-of-arrival (DOA). On the other hand, the received HF signal is very rich in information about the ionosphere which it is probing. The effects of different models of density irregularities and their positions relative to the transmitter are studied.

4.10 IAT.10: Global Thermospheric Response to Geomagnetic Storms From CHAMP Accelerometer Data – by Sutton, Eric

Status of First Author: Student in the poster competition PhD

Authors: Sutton, E. K. (eric.sutton@colorado.edu) Forbes, J. M. (forbes@colorado.edu) Nerem, R. S. (nerem@colorado.edu)

Abstract: Measurements of atmospheric density from the CHAMP satellite near 410 km are used to illustrate the dependence of latitudinal and day/night response of the thermospheric region to elevated levels of magnetic activity. The latitude vs. time evolutions of total mass density at local times near 01:00 and 13:00 hours are inferred from accelerometer measurements on the CHAMP satellite. These results are compared with density predictions from the NRLMSISE-00 empirical density model. Zonal winds near the equator along with polar north/south winds are analyzed using cross-track accelerometer measurements from CHAMP. The time period considered includes a significant geomagnetic storm from Oct 29 to Nov 1, 2003, which exhibits elevated magnetic activity of approximately Kp = 5-9. Response during this storm is compared to typical quiet-time behavior before the storm and the relaxation period directly after the storm. This time interval provides an opportunity to examine the polar Thermospheric circulation pattern observing neutral density and North/South winds during both active and quiet magnetic conditions. Day/night differences in the equatorward penetration of both global-scale and small-scale density perturbations are also examined in terms of diurnal variations in the solar-driven meridional flow.

4.11 IAT.11: Night-Time Airglow Science and All-Sky Imaging by the Penn State All-Sky Imager at Arecibo. – by Seker, Ilgin

Status of First Author: Student in the poster competition Masters

Authors: Ilgin Seker, Penn State Uni., ius102@psu.edu John D. Mathews, Penn State Uni., JDMathews@psu.edu

Abstract: The Penn-State All-Sky Imager installed in the Arecibo Observatory, PR is a high-resolution optical imager which has been collecting data at night since April, 2003. Other than the open position, it has been using 2 filters at 630nm (red), and 557.7nm(green) which correspond to oxygen emmisions in the ionosphere. A new filter at 777.4nm has recently been installed. The all-sky data taken for more than one year now, is being used to explain some ionospheric events, plasma instabilities, etc. The events in both small and large time/spatial scales are being examined and tried to be categorized. The poster is going to introduce the Penn State All-Sky Imager and present some of the important data taken from it along with brief comments.

4.12 IAT.12: Adapting Astronomical Sky Spectra for Use By the CEDAR Community. – by Sharpee, Brian

Status of First Author: Nonstudent

Authors: Brian Sharpee, SRI Int'l, brian.sharpee@sri.com David Huestis, SRI Int'l, david.huestis@sri.com Tom Slanger, SRI Int'l tom.slanger@sri.com Philip Cosby, SRI Int'l philip.cosby@sri.com

Abstract: Spectra of the night airglow captured inadvertently by astronomers comprise a vast and valuable resource for research of the middle and upper atmosphere. Presented here are the details and status of a plan to adapt astronomical sky spectra to the needs of the CEDAR community. An emphasis is placed on the development of a virtual "observatory" capable of bridging the gap between raw proprietary astronomical spectra, and immediately usable scientific data disseminated via the web.

5 Tuesday Evening 29 June 2004 Poster Session Abstracts, Equatorial thermosphere and ionosphere

5.1 EQU.01: GPS-Based Observations of the Equatorial Anomaly and F-region Irregularities over Brazil – by Rodrigues, Fabiano

Status of First Author: Student in the poster competition PhD

Authors: F. S. Rodrigues and D. L. Hysell Cornell University, USA
E. R. de Paula and M. A. Abdu Divisao de Aeronomia, DAE/INPE, Brazil

Abstract: The Brazilian National Institute for Space Research (INPE) operates two dual-frequency GPS receivers for Equatorial Anomaly (EA) and Equatorial Spread F (ESF) studies. One receiver is installed at Sao Luis (-1.73 degrees dip latitude), under the magnetic equator, while the other one is placed at Sao Jose dos Campos (-18.01 degrees dip latitude), which is located near to the nominal position of the EA peak. This poster presents first results of TEC measurements using these two receivers. Even these receivers not being located at the same magnetic longitudes, we could derive latitudinal profiles of TEC from about +5 to 25 degrees dip latitude. Profiles derived during ESF conditions show the effects of spatial gradients caused by a pronounced EA in the thin shell approximation. Additionally, we will present simultaneous measurements of L-Band scintillations caused by F-region irregularities over the Brazilian Territory.

5.2 EQU.02: Equatorial Plasma Bubble Observations from DMSP, ROCSAT-1, and CHAMP – by Burke, W presented by de La Beaujardiere, O

Status of First Author: Nonstudent

Authors: W. J. Burke, L. C. Gentile, K. Kachner, S. -Y. Su, O. de La Beaujardire
Air Force Research Laboratory, Space Vehicle directorate, Hanscom AFB, MA

Abstract: We compare evening sector observations of equatorial plasma bubbles (EPBs) from polar-orbiting Defense Meteorological Satellite Program (DMSP) satellites at 840 km with plasma densities measured by the Republic of China Satellite (ROCSAT-1) in a low-inclination (35o, 600 km) orbit and the Challenging Minisatellite Payload (CHAMP) satellite in a 90o inclination orbit at 450 km. DMSP EPB observations were acquired at low magnetic latitudes from 1989 to 2002. ROCSAT-1 plasma densities were measured in the equinox months of March and April of 2000 and 2002, and the data from CHAMP were recorded in March 2002. We first developed a climatology of EPB occurrence based on 12,000 EPB detections from 95,000 DMSP orbits. Seasonal-longitudinal variations generally agree with a model proposed by Tsunoda (1985) that predicts EPB occurrence rates should be highest when the equatorial magnetic field aligns with the dusk terminator. However, the database also reveals both unexpected phase shifts in occurrence maxima and purely longitude variations not predicted by the model. We then compared ROCSAT-1 EPB detections and statistical distributions by magnetic local time (MLT), magnetic latitude, and geographic longitude and found them well correlated with the DMSP climatology. The data suggest that energetic electrons precipitating from the inner radiation belt at eastern Pacific longitudes enhance E layer conductances and systematically decrease EPB growth rates. We are currently using a new module of AF-GEOSpace to examine multipoint observations of EPBs by the DMSP, ROCSAT-1, and CHAMP satellites at various altitudes to study EPB formation, magnitude, and duration in preparation for the Communication/Navigation Outage Forecasting System (C/NOFS) mission.
Reference: Tsunoda, R. T., JGR, 90, 447, 1985.

5.3 EQU.03: C/NOFS validation plans, and pre-C/NOFS validation results – by de La Beaujardiere, O

Status of First Author: Nonstudent

Authors: O. de La Beaujardire, J. Retterer, G. Crowley, D. Cooke, C. Valladares, F. Rich, D. Hunton, J. Welsh, J. Mellein
Air Force Research Laboratory, Space Vehicle directorate, Hanscom AFB, MA
South West Research Institute, San Antonio, TX
Boston College, MA

Abstract: The Communication/Navigation Outage Forecasting System (C/NOFS) Mission aims at specifying and forecasting the ambient ionosphere and the ionospheric scintillation in the equatorial regions. The operational objectives are to develop reliable forecasts of communication and navigation outages. The C/NOFS satellite will be launched in December 2004 into a low inclination orbit (13 degrees). Its apogee and perigee are at 710 and 375 Km, respectively. The satellite instruments include the Planar Langmuir Probe (PLP); Vector Electric Field Instrument (VEFI); Ion Velocity Meter (IVM); Neutral Wind Meter (NWM); GPS dual-frequency receiver (CORISS); Coherent radio beacon (CERTO). This poster describes the validation plans for the parameters derived from the satellite instruments, and for the models that nowcast and forecast the electron density and the scintillation. Details about ground-based and satellite-based instruments that will be used, including problems and limitations associated with the ground truth data will be presented. Preliminary plans for the validation campaigns will be shown. Results from pre-C/NOFS validation campaigns, including a simulation of the Halloween storm (Oct 29-Nov 1, 2003) will be described. Two models were run for this period: the CNOFS physics-based ionospheric model and the TIMED-GCM.

5.4 EQU.04: Midnight Temperature Maximum study from the Arequipa Fabry-Perot interferometer – by Faivre, Michael

Status of First Author: Student in the poster competition PhD

Authors: michael Faivre, faivre@clemson.edu John Meriwether, Clemson University meriwej@ces.clemson.edu, Clemson University Manfred Biondi, Pittsburg University

Abstract: The convergence of the thermospheric winds at low latitude at night produces a downwelling of air. The resulting compressional heating leads to a midnight temperature maximum (MTM)combined with significant effects on the thermospheric dynamics. A study of these effects was carried out from the Arequipa Fabry-Perot measurements for the period 1996-2002.

5.5 EQU.05: Statistical Analysis of Equatorial Spread F Activity Seen From TIMED/GUVI – by Comberiate, Joseph

Status of First Author: Student in the poster competition PhD

Authors: Joseph Comberiate, University of Illinois, comberia@uiuc.edu Julie Krekeler, University of Illinois, krekeler@uiuc.edu Farzad Kamalabadi, University of Illinois, farzadk@uiuc.edu Larry Paxton, Johns Hopkins University Applied Physics Laboratory, Larry.Paxton@jhuapl.edu Hyosub Kil, Johns Hopkins University Applied Physics Laboratory, Hyosub.Kil@jhuapl.edu

Abstract: GUVI (Global Ultraviolet Imager) brightness measurements at 1356 have been used to detect occurrences of Equatorial Spread F (ESF). Analysis of two years of GUVI data has provided statistical information about the seasonal variation of ESF occurrence in different longitude sectors of the globe as well as the corresponding characteristics of the Equatorial Ionization Anomaly (EIA). Tomographic inversion of these brightness measurements yields electron density images that are used to characterize the peak electron density values in the EIA as well as the height of the electron density peak in the F region. Past observations have identified seasons of enhanced ESF in the Atlantic, Pacific, and Indian longitude sectors. Day-to-day variations in ESF occurrence have been linked to penetrating electric fields from geomagnetic activity and asymmetric density patterns in the EIA. An automated process was developed to determine the seasonal occurrence statistics of ESF seen by GUVI in the post-sunset ionosphere. This seasonal analysis was also correlated with geomagnetic activity to study its impact on observed patterns of

ESF occurrence. Multi-dimensional inversion of GUVI data was used to reconstruct electron density profiles in both the Northern and Southern arcs of the EIA to characterize cases where asymmetry in the EIA arcs led to suppression of ESF. These results from GUVI data are presented and interpreted in the context of past work in ESF characterization.

5.6 EQU.06: Longitude Variations in Topside Equatorial Electrodynamics of the Ionosphere – by Hartman, William

Status of First Author: Student NOT in the poster competition PhD

Authors: William Hartman, University of Texas at Dallas, dhartman@hotmail.com

Abstract: The ability to model the ionosphere and predict its density and composition would benefit both navigation and communication fields. Current global models are based on the assumption that measurements from one low-latitude location are a sufficient input. In order to verify model reliability, the variables need to be tested for any longitudinal variation. DMSP, a set of sun synchronous polar orbiting satellites, was used to observe ion density and ExB drifts at four local times for one complete year during solar max. Ion density and ExB drifts were shown to be dependent on season and longitude. Therefore, present models could be improved by taking these variations into account.

5.7 EQU.07: Bottom and topside equatorial ionospheric profiles: A comparison study between IRI model and measurements over Jicamarca – by Ilma, Ronald

Status of First Author: Nonstudent

Authors: Ronald R. Ilma and Jorge L. Chau, Radio Observatorio de Jicamarca, Instituto Geofisico del Per **Abstract**: Incoherent scatter radars (ISRs) and ionosondes are powerful and complementary techniques in the study of the Earths ionosphere. The work presented here concerns the analysis and validation of electron densities profiles generated with IRI 2000 (International Reference Ionosphere) model and data collected with both the ionosonde and the ISR located at Jicamarca, Peru (11.95 deg S, 76.87 deg W). While the latter one can observe above the F peak, the ionosonde only measures the bottomside. In order to estimate the electron density profile above the F2 layer peak, the ionosonde approximate the topside profile by a Chapman function with information that is derived from the bottomside. Our preliminary results compared to the ISR profiles show (1) very good agreement at the bottomside with both Ionosonde and IRI, (2) good agreement with inferred ionosonde topside below 800 kms, above this height there is a persistent underestimation, and (3) poor agreement with IRI profiles in the topside (overestimation). Based on these results we proposed that the topside functions of IRI, particularly at equatorial latitudes should be revisited.

5.8 EQU.08: Bubbles as ducts for the equatorward flow of thermospheric composition disturbance – by Kil, Hyosub

Status of First Author: Nonstudent

Authors: Larry Paxton, JHU/APL, larry.paxton@jhuapl.edu, Shin-Yi Su, NCU, Taiwan, t2700146@ncu865.ncu.edu.tw, Yongliang Zhang, JHU/APL, yongliang.zhang@jhuapl.edu, H. C. Yeh, NCU, Taiwan, hcyeh@jupiter.ss.ncu.edu.tw, Brian Wolven, JHU/APL, brian.wolven@jhuapl.edu Danny Morrison, JHU/APL, danny.morrison@jhuapl.edu

Abstract: Several storm-induced big bubbles (SIBBs) are detected during the magnetic storms of JUly 15, 2000, March 31, 2001, October 29, 2003, and November 20, 2003. SIBBs occur in the equatorial region during nighttime, are elongated in the north-south direction, have steep walls, and co-existed with plasma bubbles. These observations corroborate that the SIBBs are associated with bubbles. We will discuss the characteristics of the SIBBs and the formation mechanism of the SIBBs from the bubbles.

5.9 EQU.09: Gravity waves seeding Spread F. – by Kohen, Talia

Status of First Author: Student in the poster competition Undergraduate

Authors: **Abstract**: We have examined several nights of Hawaiian airglow data in search of evidence for gravity wave seeding of Convective Ionospheric Storms, aka Equatorial Spread F. Nights with and without bubbles are examined for all four seasons. The results are at the moment ambiguous.

5.10 EQU.10: Response of the Equatorial Ionization Anomaly during Disturbance Periods in Different Seasons: Observation and Model Results – by Lin, Charles

Status of First Author: Student in the poster competition PhD

Authors: C. H. Lin (clin@ucar.edu) High Altitude Observatory, NCAR, P. O. Box 3000, Boulder, CO 80307, USA Institute of Space Science, National Central University, Chung-Li 320, Taiwan A. D. Richmond (richmond@ucar.edu) High Altitude Observatory, NCAR, P. O. Box 3000, Boulder, CO 80307, USA G. J. Bailey (G.Bailey@sheffield.ac.uk) Department of Applied Mathmatics, University of Sheffield, Sheffield S3 7RH, UK J. Y. Liu (jyliu@ss.ncu.edu.tw) Institute of Space Science, National Central University, Chung-Li 320, Taiwan

Abstract: A chain of ground based GPS receivers that cover from -60 to 60 degree magnetic latitude in the American sector (along 290 degree W geographic longitudinal line) has been used to observe the storm time variation of the equatorial ionization anomaly (EIA). From the observation results, the daytime EIA shows great expansion in latitudinal extent with the TEC enhancement right after the storm sudden commencement (SSC). This expansion may due to the storm produced eastward electric field that penetrates from the magnetosphere to the ionosphere and thus enhances the low latitude ionosphere plasma fountain. After the expansion phase, the EIA often shows contraction and depletion features during the second day of the storm. Meanwhile, the observation results also show that the EIA becomes more asymmetric during the depletion phase in different seasons. To better understand the interplay of the storm produced electric field, neutral wind, and composition changes in different seasons, we perform model runs to compare with the observation results.

5.11 EQU.11: Microbarometric Studies of Atmospheric Pressure Variations – by Livneh, Dorey

Status of First Author: Student in the poster competition PhD

Authors: Dorey J. Livneh: dul121@psu.edu John Mathews: JDMathews@psu.edu
Both are from the Pennsylvania State University

Abstract: Microbarometric Studies of Atmospheric Pressure Variations
Dorey Livneh, John D. Mathews.
A microbarometer is set up at Arecibo Observatory in Puerto Rico and has been collecting data on atmospheric pressure variations since mid March of 2003. This data will be used, along with ionospheric (incoherent scatter radar), seismic and all-sky optical observations in an attempt to more comprehensively understand the role of atmospheric waves observed in the lower atmosphere on upper atmosphere/ionosphere processes. Another microbarograph is to be set up roughly 100 km away to distinguish between local and longer varying wave phenomena and to establish horizontal correlation distances.

5.12 EQU.12: Inter-Hemispheric Comparisons of the Latitude Extent of Thermosphere-Ionosphere Disturbances – by Martinis, Carlos

Status of First Author: Student in the poster competition PhD

Authors: J.Wroten, jwroten@bu.edu J.Baumgardner, jeffreyb@bu.edu S.M.Smith, smsms@bu.edu M.Mendillo, mendillo@bu.edu Center for Space Physics- Boston University

Abstract: All-sky imagers located at Arecibo, Puerto Rico (18.3 N, 66.7 W, 28 N mag) and El Leoncito, Argentina (31.8 S, 69.3 W, 18 S mag), are used to compare 630.0 nm airglow emission features. Airglow depletions associated with Rayleigh-Taylor instability (ESF) and brightness waves associated with the midnight temperature maximum (MTM) are frequently observed at both sites. While not at conjugate points, these two sites allow the evaluation of statistical occurrence patterns and, simultaneous case-study events from the same longitude sector in both hemispheres. While both types of disturbances are well studied at near-equatorial latitudes (L around 1.1), we find the intrusion of those processes to lower-mid latitudes (L around 1.35) on a relatively frequent basis. The traditional role of latitude coupling (from high to low-latitude) needs to be expanded to study how equatorial aeronomy phenomena reach into mid-latitude domain.

5.13 EQU.13: Effect of the Direct Penetration Electric Field on the Disturbance Dynamo, and the Storm-time Equatorial Ionosphere and Thermosphere – by Maruyama, Naomi

Status of First Author: Nonstudent

Authors: N. Maruyama (naomi@ucar.edu, HAO/NCAR), T.J. Fuller-Rowell (tim.fuller-rowell@noaa.gov, SEC/NOAA and CIRES/University of Colorado), M. Codrescu (mihail.codrescu@noaa.gov, SEC/NOAA and CIRES/University of Colorado), A.D. Richmond (richmond@ucar.edu, HAO/NCAR), G. Millward (george@apl.ucl.ac.uk, University College London, UK), R.W. Spiro (spiro@rice.edu, Rice University), S. Sazykin (sazykin@rice.edu, Rice University), F. Toffoletto (toffo@rice.edu, Rice University), and C. Lin (clin@ucar.edu, HAO/NCAR) **Abstract**: The direct penetration of the high-latitude electric field to lower latitudes, and the disturbance dynamo, both play a significant role in restructuring the storm-time equatorial ionosphere and thermosphere. The fundamental mechanisms of each disturbance electric field are understood. However, in a particular observation of the equatorial electric field, it has been difficult to actually identify the source, determine the relative importance of the two mechanisms, and associate the source with the changes in the ionosphere and thermosphere. This study utilizes the Coupled Thermosphere-Ionosphere-Plasmasphere-Electrodynamics (CTIPe) model, in which the mid and low-latitude electrodynamics is solved self-consistently with the global ionosphere-thermosphere system. In order to investigate the effect of the direct penetration electric field together with the disturbance dynamo process on the equatorial ionosphere and thermosphere, the Rice Convection Model (RCM) electric fields are imposed on CTIPe. Our results show that the direct penetration electric field can modify the ionospheric dynamo by changing the conductivity and neutral wind. We discuss our results in relation to observations of low-latitude ionospheric disturbances.

5.14 EQU.14: MEASUREMENT OF SPREAD F USING A NETWORK OF GPS RECEIVERS IN COLOMBIA – by Patino, Erika

Status of First Author: Student in the poster competition Masters

Authors: Erika Patino, Cesar Perez, Sebastion Olarte, Carlos Herrera, Alfonso Devia, Jaime Villalobos, Universidad Nacional de Colombia Cesar E. Valladares, Institute for Scientific Research, Boston College

Abstract: Two GPS receivers have been situated 166 km apart in a mainly East-West directed baseline. One of the receivers is located at Bogota (4.63 N, 74.08 W) and the other at Manizales (5.03 N, 75.47 W) The scientific goal of this project is to study the characteristics of the local ionosphere including plasma irregularities, GPS scintillation behavior, and total electron content (TEC) depletions, as well as the evolution of the anomaly and plasma stabilities. Calculations of monthly average of scintillation duration for the months of March and April 2004 will also be presented

5.15 EQU.15: Daytime vertical and zonal velocities from 150-km echoes over Jicamarca – by Chau, Jorge presented by Scipion, Danny

Status of First Author: Nonstudent PhD

Authors: Jorge L. Chau - Radio Observatorio de Jicamarca, Instituto Geofsico del Per, Lima, Per - jchau@jro.igp.gob.pe Ronald F. Woodman - Radio Observatorio de Jicamarca, Instituto Geofsico del Per, Lima, Per - ronw@geo.igp.gob.pe Danny E. Scipion - Radio Observatorio de Jicamarca, Instituto Geofsico del Per, Lima, Per - dscipion@jro.igp.gob.pe

Abstract: As it was suggested by Kudeki and Fawcett [1993] and later shown by Woodman and Villanueva [1995], the Doppler velocities of 150-km echoes represent the vertical ExB drift velocities at F region altitudes. Although we still do not have a complete understanding of the irregularity mechanism, 150-km observations represent an excellent mean of monitoring the electric fields at equatorial latitudes. Low power observations of 150-km echoes using the JULIA system have been carried out almost continuously since August 2001 at Jicamarca [e.g., Anderson et al., 2004]. Most of the observations have been done pointing perpendicular to the magnetic field (B) in the magnetic meridian, allowing the measurement of the vertical component of the ExB drift. However, few campaigns have been carried out with the JULIA system using two oblique beams. With this two-beam configuration we are able to measure the zonal velocity component. In order to understand the significance of this new parameter (i.e., the zonal velocity around 150 km during the day at equatorial latitudes) a special experiment has been conducted to obtain concurrently velocities from 150-km echoes and from the east-west drift incoherent scatter radar (ISR) mode perpendicular to B [e.g., Kudeki et al., 1999]. From these comparisons (1) we have verified the excellent correlation between their vertical components, i.e., 150-km vertical velocities represent the ionospheric ExB vertical drift, and (2) there is a poor agreement between their zonal components (correlation ¡ 0.7). The latter result should not be surprising since the F region is strongly coupled to the E region owing to the high conductivity along the magnetic field lines. The E region itself represent high conductivity so the F region and also the region around 150 km responds to the electric filed imposed by the E region. Therefore the observed zonal velocities from 150-km echoes could be an indication of the zonal neutral winds at E region heights few degrees away from the magnetic equator.

5.16 EQU.16: Plasma bubble zonal velocity variations with solar activity over the Brazilian region – by Terra, Pedrina

Status of First Author: Student NOT in the poster competition PhD

Authors: Terra, Pedrina Morais dos Santos-INPE-pedrina@dae.inpe.br; Sobral, Jos Humberto Andrade-INPE-sobral@dae.inpe.br; Abdu, Mangalathayil Ali-INPE-abdu@dae.inpe.br; Souza, Jonas Rodrigues de-INPE-jonas@dae.inpe.br; Takahashi, Hisao-INPE-takahashi@laser.inpe.br; Brum, Christiano Garnett Marques-INPE-garnett@dae.inpe.br

Abstract: A statistical study of the zonal drift velocities of the ionospheric plasma bubbles using experimental airglow data acquired at the low-latitude station Cachoeira Paulista (Geogr. 22.5S, 45W, dip angle 28S) during the period of October to March, between 1980 and 1994, is presented here. This study is based on 109 nights of zonal plasma bubble velocity estimations as determined from bubbles signatures on the OI 630 nm scanning photometer airglow data. The zonal velocity magnitudes of the plasma bubbles are investigated with respect to solar activity and local time. It is verified that these velocities tend to increase with the solar EUV flux, using the solar 10.7-cm radio flux as a proxy (F10.7). These velocities are seen to be larger during the solar maximum activity period than in the solar minimum period. As to the local time variation, they are seen to peak before midnight, in the 20:30 - 22:30 LT time frame, depending on the season. The all-data plot based on the 109 nights of airglow experiments shows that the plasma bubble mean zonal drift velocities tend to decrease with local time, but they peak at 22:25 LT where the velocity magnitude reaches 127.4 ms-1. The zonal drift accelerations with local time and solar flux are shown in Figures 1 and 2, respectively.

5.17 EQU.17: A comparison of the characteristics of the observed and modeled equatorial anomaly – by Valladares, Cesar

Status of First Author: Nonstudent

Authors: C.E. Valladares, Boston College valladar@bc.edu V. Eccles, J. Chau, Jicamarca Radio Observatory, chau@jro.igp.gob.pe

Abstract: The equatorial anomaly (also named Appleton anomaly) is an almost permanent feature of the low latitude ionosphere that usually develops during the early morning and persists even after sunset. We have used the LLIONS (IFM) model to simulate the development of the equatorial anomaly. The numerical model is driven using the vertical drifts measured at Jicamarca on 49 world days between 2001 and 2003. Then, we have compared the characteristics of the modeled anomaly with the properties of the real anomaly as measured by the network of GPS receivers in South America and a digisonde located at Jicamarca. This study aims (1) To investigate the relationship between the hmF2, NmF2, latitude of the crests, the driving vertical drift, and the ratio of the TEC values at the crest and at the trough. (2) To examine the agreement between the observed and the modeled TEC latitudinal profiles. (3) To assess the importance of the meridional wind (and other factors such as the altitude dependence of the vertical drift) for improving the agreement between the modeled and the observed TEC values. It was found that between the early morning and the afternoon hours (9-21 UT) the relationship between the vertical velocity, the hmF2 and the displacement of the crests is close to linear. However, at later local times the proportionality becomes more complex. The importance of this study resides in the close relationship between a full development of the anomaly and the onset and persistence of equatorial spread F.

5.18 EQU.18: Generation of Metastable Helium and the 1083 nm Emission in the Upper Thermosphere – by Waldrop, Lara

Status of First Author: Nonstudent

Authors: L. Waldrop (University of Illinois, lwaldrop@uiuc.edu), R. Kerr (Dartmouth College), S. Gonzalez (Arecibo Observatory), M. Sulzer (Arecibo Observatory), J. Noto (Scientific Solutions, Inc.), E. Kudeki (University of Illinois). F. Kamalabadi (University of Illinois) **Abstract**: Models of metastable helium production in the upper thermosphere and lower exosphere over Arecibo show that creation by recombination of He+ can be non-negligible relative to the photoelectron impact on ground state Helium source. Due to large ground-state He abundance in the winter, and to photoelectrons from an illuminated conjugate thermosphere, the strongest 1083 nm intensities (arising from solar resonance) occur during the winter. The contribution to the 1083 nm airglow brightness from He+ recombination reaches more than 10% in the morning twilight when He+ peak concentrations are more than 30% of the topside composition, and He+ recombination becomes increasingly dominant for solar zenith angles greater than 110 degrees. Measurements of the topside ionosphere at Arecibo have shown that He+ layer concentrations in the winter and near the equinoxes are often as high as 50% and significant He+ concentrations can persist throughout the night. A hot metastable component from recombination renders ambiguous interpretation of the 1083 nm spectral profile in terms of exospheric temperature. The presence of such a population may explain reported observations of 1083 nm line widths that increase with shadow height, implying twilight temperatures much hotter than those expected of a thermalized neutral population. Modeling of 1083 nm line profiles comprised of both thermal and nonthermal metastable Helium components is investigated to assess the role of He+ recombination in the generation of metastable He and the implications for the derivation of neutral temperature in the upper thermosphere.

6 Tuesday Evening 29 June 2004 Poster Session Abstracts, Magnetosphere-ionosphere coupling

6.1 MIC.01: Experimental data and modelling of ionospheric TEC during the 21st October 2001 storm. – by Denton, Michael

Status of First Author: Nonstudent

Authors: M. H. Denton(1), D. Malan(2), M. F. Thomsen(1), G. J. Bailey(3), S. E. Pryse(2)
1) Los Alamos National Laboratory, Los Alamos, NM 87544, USA 2) University of Wales, Aberystwyth, UK 3) Universtiy of Sheffield, Sheffield, UK

Abstract: We use a combination of magnetospheric and ionospheric experimental data to examine the storm of 21st October 2001. During this storm, steep gradients were observed in the ionospheric total electron content (TEC) at mid- and high-latitudes. Examination of data from geosynchronous orbit, indicate that this storm was a 'sawtooth' event, characterised by a repeated series of substorms during each of which plasma was injected from the plasma sheet into the inner magnetosphere. At high latitudes these injections cause enhanced auroral activity. We use the SUPIM (Sheffield University Plasmasphere Ionosphere Model) and CTIP (Coupled Thermosphere Ionosphere Plasmasphere Model) theoretical models to show the expected global response to the storm, and compare with experimental data to examine the effects in the mid- and high-latitude ionosphere.

6.2 MIC.02: High Energy Proton and Electron Precipitation in the April 2002 storms – by Fang, Xiaohua

Status of First Author: Student in the poster competition PhD

Authors: Xiaohua Fang (University of Michigan, xhfang@umich.edu), Janet Kozyra (University of Michigan, jukozyra@umich.edu), Michael Liemohn (University of Michigan, liemohn@umich.edu), Aaron Ridley (University of Michigan, ridley@umich.edu), David Evans (SEC/NOAA, David.S.Evans@noaa.gov), Stanley Solomon (HAO/NCAR, stans@ucar.edu)

Abstract: Precipitating electrons and protons from the magnetosphere are a major energy source in the high latitude region of the Earth. The spatial and temporal variations of energetic particle impacts in a global view are of importance in our understanding of the magnetospheric activities in source regions and their resulting ionospheric and thermospheric perturbations. Time averaged NOAA POES satellite data provide a global picture of energetic proton precipitation pattern by data integration and interpolation over 3-hour intervals during the April 2002 magnetic storms. The resulting ionospheric electron density distribution by incident energetic protons are obtained from a three-dimensional Monte Carlo ion precipitation model. Simulation results for energetic electrons are presented as well, using a new global ionosphere thermosphere model (GITM) with input from AMIE. The spatial and temporal variations of the relative contributions from energetic proton and electron precipitation are examined during the April 2002 storm period.

6.3 MIC.03: Neutral Polar Wind – by Gardner, Larry

Status of First Author: Student in the poster competition PhD

Authors: Larry C. Gardner, Center for Atmospheric and Space Sciences, Utah State University, Logan, Utah, USA emphyx@yahoo.com
Robert W. Schunk, Center for Atmospheric and Space Sciences, Utah State University, Logan, Utah, USA robert.schunk@usu.edu

Abstract: The classical polar wind is an ambipolar outflow of ions from high latitudes along open geomagnetic field lines. The polar wind consists of light thermal ions (H+, He+) and energetic light and

heavy ions (H+, He+, O+). The characteristics of these ions have been studied quite extensively since the 1960s. In just the last 20 years, however, energetic neutral atoms (ENAs) that are produced in charge exchange reactions between the singly ionized polar wind ions and the surrounding neutral atoms have been used as a means to remotely probe plasma populations. A theoretical model has been used in this study that is similar to the high-latitude hydrodynamic polar wind model developed at Utah State University, but it has been expanded to include the effects of neutral stream particles so that the characteristics of the neutral polar wind can be elucidated.

6.4 MIC.04: Meso-scale Velocity Structure in the High-Latitude F Region – by Johnson, Eric

Status of First Author: Student in the poster competition PhD

Authors: Eric S. Johnson, The University of Texas at Dallas, ejohnson@utdallas.edu R.A. Heelis, The University of Texas at Dallas, heelis@utdallas.edu

Abstract: At high latitudes in the F region the bulk ion flow is driven predominantly by electric fields originating in the magnetosphere and magnetosheath. During times of southward IMF a large-scale 2-cell convection pattern usually prevails with characteristic spatial scales of 1000 km (10 degrees of latitude). In addition to this large-scale convection feature there exist smaller scale velocity structures with scale sizes ranging from 100's of km to 10's of meters. At intermediate scales between 10 km and 1000 km the ion velocity structure can have a significant impact on the ion temperature and perhaps the neutral gas velocity. Here we report on an initial study of the characteristics of ion velocity structure in this scale size range. We examine the characteristics of structure in the auroral zone and polar cap in the winter and summer hemispheres during times of southward IMF. We also consider relationships between the intermediate scale size structure and the magnitude of large-scale gradients in the bulk flow.

6.5 MIC.05: Dayside Ion Upwelling During Solar Maximum at Svalbard: Background, Statistical and Case Studies – by Remick, Karen

Status of First Author: Student NOT in the poster competition PhD

Authors: **Abstract**: The dayside cusp region is a dominant source for O+. The atmospheric conditions that are associated with ion upwelling above Svalbard are examined in this study. The average values for Ne, Te, Ti, Vi and ion flux are determined. Statistical and case studies are made to determine which parameter upward ion acceleration is related to.

6.6 MIC.06: The Global Ionosphere Thermosphere Model Results of the April 2002 Storm – by Ridley, A.

Status of First Author: Nonstudent

Authors: A. Ridley, G. Toth, Y. Deng, J. Kozyra, all of the University of Michigan, T. Immel, University of California Berkeley, and L. Paxton, Johns Hopkins University Applied Physics Laboratory

Abstract: We present results from a new global ionosphere thermosphere model (GITM). The model is a self-consistent first-principles models of the coupled ionosphere thermosphere system from 95 km to 700+ km. GITM solves for the non-hydrostatic thermospheric state in altitude coordinates, having a stretched grid in both the altitude and latitude directions. The high-latitude electrodynamics are specified by input from AMIE, while the low-latitude electrodynamics are controlled by the self-consistent coupling between the ion and neutral flows. We present thermospheric and ionospheric results from the April 2002 storm period, comparing those results to observations from global imagers and measurements of NO. We further show the effects of small-scale structures in the aurora and ion flows on the global solution.

6.7 MIC.07: Plasma and electromagnetic structures in the mid-latitude ionosphere caused by the magnetosphere-ionosphere interaction. – by Streltsov, Anatoly

Status of First Author: Nonstudent PhD

Authors: Anatoly V. Streltsov, Dartmouth College, streltsov@dartmouth.edu

Abstract: Dynamics of intense, localized structures in the electric field, current, and plasma density observed inside and above the nightside, mid-latitude ionosphere are investigated numerically. It is suggested that these structures are generated in the process of the magnetosphere-ionosphere coupling mediated by the dynamics of magnetic field-aligned currents (FACs). Field-aligned currents represent shear Alfven waves standing or propagating along the ambient magnetic field between the conjugate ionospheres. In case when the background ionospheric conductivity is low, and the large-scale electric field exists inside the ionospheric E-layer, interaction between FACs and the ionosphere can increase the magnitude of the reflected current and induce variation of the ionospheric density. This active ionospheric feedback on the structure and amplitude of the FAC interacting with the ionosphere may lead to a so-called ionospheric feedback instability. Properties of this instability are investigated numerically depending on the parameters of the mid-latitude ionosphere, magnetosphere, and the field-aligned current system.

7 Tuesday Evening 29 June 2004 Poster Session Abstracts, Meteor science (other than winds)

7.1 MET.01: Up In Smoke? UHF RADAR Meteor Observations and the Terminal Event – by Briczinski, S

Status of First Author: Student in the poster competition PhD

Authors: S. J. Briczinski, Penn State, sjb144@psu.edu J.D. Mathews, Penn State, jdmathews@psu.edu D.D. Meisel, SUNY Geneseo, meisel@geneseo.edu

Abstract: The micrometeor observations performed using the 430 MHz Arecibo Observatory radar have proven to be crucial for the understanding of meteoric effects on the aeronomy of the upper atmosphere. Previous techniques using the Arecibo radar have required manual confirmation of each event, followed by direct measurements of the parameters (i.e. altitudes, velocities and deceleratons). Observations of sporadic (non-shower) meteors during February of 2001 have been analyzed with an FFT periodic search algorithm that automatically detects meteor events between altitudes of 85 and 125 km. We present the new technique used to detect meteors as well as the measured parameters obtained from this method. The results of the new automated technique are compared with previous results. This new technique shows an improvement over traditional searching routines by increasing the event rate by as much as 30%. In some cases meteor events are observed that appear to catastrophically destruct within the beam. These events may undergo minor ablation of their volatile components before annihilation 'the terminal event' that occurs in under 1 ms. As with essentially all observed meteoroids, the meteoroids that disappear in a terminal event appear to experience linear decelerations before their abrupt disappearance. This non-ablative mass deposition process may play an important role in the composition of the upper atmosphere as it apparently produces sub-micron sized particles. We present the meteor parameters obtained from an automatic FFT meteor searching routine and consider the terminal-event destruction of meteoroids and resultant mass deposition as an important factor in the aeronomy of the meteor zone. Calculations of meteroid orbital parameters are also presented. We discuss the discovery of new extra-solar particles incident on the atmosphere. We also present the first results on the altitude, speed, and mass distributions of terminal event meteoroids yielding some clues on the physics of the terminal-event.

7.2 MET.02: Diurnal Variability of Specular and Non-specular Radar Meteor Trails – by Denney, Kelly

Status of First Author: Student in the poster competition Undergraduate

Authors: Kelly Denney, Lars P. Dyrud, Erhan Kudeki, Julio Urbina, Diego Janches, Meers Oppenheim

Abstract: We used radar observations from the Coqui II 50 MHz radar, located near Salinas, Puerto Rico, to measure observed counts of both specular and non-specular meteor trails in the E-region ionosphere. These observations were made over a time span ranging from 18:00 to 08:00 on various days in 1998 and 1999. The Coqui II radar has two sub-arrays, both pointed to the north in the magnetic meridian plane, perpendicular to the magnetic field, at an elevation angle of approximately 41 degrees. Traditional meteor radars require trail specularity (trail perpendicular to radar beam) for a reflection, but over the past decade, two new types of radar meteor reflections, known as meteor head echoes and non-specular trails, have become known or widely used. Many estimates for determining global meteor mass flux have used these traditional meteor radars counting only specular meteor trails. To determine the extent that specular trails represent a non-biased, full spectrum observation of the meteor flux, we examine the diurnal variability of specular trails versus non-specular trails. We use common volume observations of these two types of meteor reflections from the same radar to show that the diurnal variability of specular trails and non-specular trails are not equivalent. Therefore, through statistical analysis of observed meteor trails of all types of reflections, we hope to better understand radar sensitivity to various aspects of meteor flux as well as gain better estimates of the this flux.

7.3 MET.03: On the Search of HyperSpeed Meteor – by Wen, Chun-Hsien

Status of First Author: Student NOT in the poster competition PhD

Authors: Chun-Hsien Wen, Penn State University, cxw381@psu.edu John F. Doherty, Penn State University, jfd6@psu.edu John D. Mathews, Penn State University, jdmathews@psu.edu

Abstract: As part of an NSF Information Technology Research (ITR) project, we present recent results on the search of hyperspeed meteors in this poster. The hyperspeed meteor is defined as the speed of the meteor is above 72 km/sec. We analyze the meteor observation data from Arecibo Observatory. Meteor Return Signature (MRS) detection algorithm, which we proposed two years ago with moderate modifications is used. We put two consecutive inter-pulse period (IPP) signals together and get the frequency spectrum by the FFT. Then we pass the frequency spectrum through a MRS correlator to detect the presence of the meteor. Experimental results show that we detect the MRS at high Doppler frequency band (corresponding speed is above 72 km/sec) in some data sets, which may suggest the existence of hyperspeed meteors.

8 Tuesday Evening 29 June 2004 Poster Session Abstracts, Solar-planetary interactions in the Earth's upper atmosphere

8.1 SPI.01: Influence of solar flux variations and geomagnetic activity on the atomic oxygen diurnal emissions in the thermosphere. – by Culot, Frederic

Status of First Author: Student in the poster competition PhD

Authors: F. Culot - LPG - frederic.culot@obs.ujf-grenoble.fr C. Lathuillere - LPG - Chantal.Lathuillere@obs.ujf-grenoble.fr J. Lilensten - LPG - Jean.Lilensten@obs.ujf-grenoble.fr

Abstract: Studying the atmosphere's airglow emissions provides valuable information about the chemical and dynamical processes controlling the state of the upper mesosphere and lower thermosphere. Reaching a better understanding of how the airglow fluctuates with respect to solar flux variations and magnetic disturbances would lead to a better knowledge of the high atmosphere response to solar and geomagnetic activity. In this perspective, a complementary approach, involving statistical analysis of measurements together with the modelling of oxygen emissions, allows us to quantify the influence of different geophysical parameters on the 630.0 nm dayglow and on the thermospheric peak of the 557.7 nm dayglow.
For the solar flux influence, a statistical analysis over 5 years of WINDII measurements (space interferometer on board NASA UARS) is performed. The volume emission rate variations due to solar flux are quantified and it is found that the intensity and altitude of both emissions increase quasi-linearly with solar flux. It is also shown that the correlations between these emission parameters and the MgII proxy are better than when the f10.7 index is used. The 1-D fluid/kinetic model TRANSCAR was used to model those dayglow variations, and the results indicates that our model appropriately reproduces the interferometer measurements all along the satellite orbit.
Concerning the geomagnetic influence, the same modelling approach was performed, allowing to evaluate the expected variations of the contributions involved in the oxygen emissions. When magnetic activity increases, the altitude of both emissions are found to be increasing, the intensity of the 557.7 nm thermospheric peak decreases, and the red line intensity is almost constant. Those trends are confirmed when analysing the WINDII green and red line measurements.

8.2 SPI.02: Coupled Model Simulation of CME Effects on the Geospace Environment – by Goodrich, C. presented by Burns, Alan

Status of First Author: Nonstudent

Authors: C. C. Goodrich, W. J. Hughes, J. A. Linker, J. G. Luhmann, J. G. Lyon, Z. Mikic, D. Odstrcil, S. C. Solomon, W. Wang, M. Wiltberger, and A. G. Burns

Abstract: This paper describes the 3D simulation of a space weather event using the coupled model approach adopted by the Center for Integrated Space Weather Modeling (CISM). The simulation employs corona, solar wind, and magnetosphere MHD models, and an upper atmosphere/ionosphere fluid dynamic model, with interfaces that exchange parameters specifying each component of the connected solar terrestrial system. A hypothetical coronal mass ejection is launched from the Sun by a process emulating photospheric field changes such as are observed with solar magnetographs. The associated ejected magnetic flux rope propagates into a realistically structured solar wind, producing a leading interplanetary shock, sheath, and magnetic cloud. These reach 1 AU where the solar wind and interplanetary magnetic field parameters are used to drive the magnetosphere-ionosphere-thermosphere coupled model in the same manner as upstream in-situ measurements. The simulated magnetosphere responds with a magnetic storm, producing enhanced convection and auroral energy inputs to the upper atmosphere/ionosphere. These results demonstrate the potential for future studies using a modular, systemic numerical modeling approach to space weather research and forecasting.

8.3 SPI.03: Satellite drag as a teaching tool for understanding the upper atmosphere – by Knipp, Delores

Status of First Author: Nonstudent

Authors: Delores Knipp, USAFA Gil Moore Judith Lean, NRL

Abstract: The SATRSHINE satellites were placed on orbit during the latest solar maximum. We use data acquired from the satellite along with a simple spreadsheet program to teach the basic physics of satellite drag and to derive information about the temperature and density structure and variation of the atmosphere below 500 km. We will provide the spreadsheet program and teaching examples to interested CEDAR participants.

8.4 SPI.04: An Analysis of the Momentum Forcing in the High-latitude Lower Thermosphere Based on the NCAR-TIEGCM: Dependence on the Interplanetary Magnetic Field (IMF) – by Kwak, Young-Sil

Status of First Author: Student in the poster competition PhD

Authors: Young-Sil Kwak, Kyungpook National University, Daegu, Korea, ys-kwak@hanmail.net Arthur D. Richmond, NCAR, High Altitude Observatory, Boulder, CO, USA, richmond@hao.ucar.edu Byung-Ho Ahn, Kyungpook National University, Daegu, Korea, bhahn@knu.ac.kr

Abstract: Lower thermospheric winds are forced primarily by non-uniform solar heating, atmospheric tides and other waves coming from below, and energy and momentum sources associated with high-latitude magnetosphere-ionosphere coupling. To understand the physical processes that control the high-latitude lower thermospheric dynamics, we quantify the forces that are mainly responsible for maintaining the high-latitude lower thermospheric wind system, and we also examine the resulting momentum balance with the aid of the National Center for Atmospheric Research Thermosphere-Ionosphere Electrodynamics General Circulation Model (NCAR-TIEGCM). Momentum forcing is statistically analyzed in magnetic coordinates, and its behavior with respect to the magnitude and orientation of the interplanetary magnetic field (IMF) is further examined in this study. Differences between winds and forces for different IMF orientations are analyzed. In the high-latitude lower thermosphere the wind tendency is large in the vicinity of the magnetic polar cap/auroral zone boundary. At higher altitudes of the lower thermosphere the primary force balance is established between Pedersen ion drag force, which creates rotational motion, and pressure; however, at various locations and times significant contributions can be made by Coriolis and horizontal advection forces. On the other hand, at lower altitudes geostrophic balance tends to dominate with a general balance between the pressure gradient and Coriolis forces. Although it is weak, the Hall ion drag force, which creates non-rotational motion, still modulates the wind tendency. The ion drag force tends to generate a warm anticyclonic or a cold cyclonic circulation on the polar cap region for negative IMF-By or positive IMF-By conditions, respectively. The ion drag, Coriolis, and pressure gradient forces are generally in balance in the polar region, with momentum advection enhancing the strength of the wind tendency in the dawn sector and diminishing it in the dusk sector, respectively.

8.5 SPI.05: The Global Ionospheric Response To Interplanetary Electric Fields Measured by Ground and Space-Borne GPS Receivers – by Mannucci, Anthony

Status of First Author: Nonstudent

Authors: ANTHONY J. MANNUCCI Tony.Mannucci@jpl.nasa.gov BRUCE T. TSURUTANI Bruce.T.Tsurutani@jpl.nasa.gov BYRON A. IIJIMA Byron.Iijima@jpl.nasa.gov ATTILA KOMJATHY Attila.Komjathy@jpl.nasa.gov GEORGE HAJJ George.Hajj@jpl.nasa.gov Jet Propulsion Laboratory, California Institute of Technology
WALTER D. GONZALEZ gonzalez@dge.inpe.br FERNANDO GUARNIERI guarnier@dge.inpe.br Instituto Nacional de Pesquisas Espaciais, Sao Jose Dos Campos, Brazil

Abstract: We will present the global ionospheric response to selected intense southward Bz interplanetary magnetic field events recorded over the last two years. Using data obtained from ground and space-borne Global Positioning System (GPS) receivers, and other data, we show evidence for global-scale, dayside ionospheric uplift soon after IMF southward turning. Increases in column-integrated electron density are observed from instrument altitudes below and within the ionosphere, during daytime over a broad latitudinal range extending from equatorial to greater than 50 degrees magnetic. The apparently prompt, coherent global-scale ionospheric response to interplanetary forcing is a very significant aspect of space weather and these new GPS datasets allow us to understand the solar wind-ionosphere coupling in greater detail than has been possible in the past.

8.6 SPI.06: Observations of Solar Cyclical Variations in Geocoronal H-alpha Column Emission Intensities – by Nossal, Susan

Status of First Author: Nonstudent

Authors: S.M. Nossal, Dept. of Physics, University of Wisconsin, nossal@wisp.physics.wisc.edu F.L. Roesler, Dept. of Physics, University of Wisconsin, roesler@wisp.physics.wisc.edu; E.J. Mierkiewicz, Dept. of Physics, University of Wisconsin, emierk@wisp.physics.wisc.edu; R.J. Reynolds, Dept. of Astronomy, University of Wisconsin reynolds@astro.wisc.edu

Abstract: Understanding the influence of the solar cycle variation on the Earths upper atmosphere is important for determining the basic state of the region, as well as for distinguishing between natural variability and possible longer term climatic trends. Geocoronal hydrogen is the byproduct of middle and upper atmospheric chemical and photolysis reactions involving its hydrogenous source species below such as methane, water vapor, and molecular hydrogen. Observations of thermospheric + exospheric H-alpha column emission by the Wisconsin H-alpha Mapper (WHAM) Fabry-Perot show a statistically significant solar cyclic variation, with higher intensities seen during solar maximum periods. We will discuss requirements for long term Fabry-Perot H-alpha observations and present comparisons from the present solar cycle (cycle 23) and between solar cycles. We will also describe how we account for correction factors in our efforts to isolate possible solar cyclic and long term trends in our observations.

8.7 SPI.07: A LOW FREQUENCY ARRAY FOR SPACE WEATHER OBSERVATIONS – by Salah, Joseph

Status of First Author: Nonstudent

Authors: Joseph E. Salah (MIT Haystack Observatory) jsalah@haystack.mit.edu Divya Oberoi (MIT Haystack Observatory) doberoi@haystack.mit.edu Justin Kasper (MIT Center for Space Reseaerch) jck@space.mit.edu

Abstract: A new generation of digital radio arrays is being designed to improve the sensitivity and resolution of astronomical and heliospheric observations, with emphasis on frequencies below 300 MHz. MIT Haystack Observatory has been engaged in the development of such an array over the past two years, and a demonstrator system is now being considered for deployment in Western Australia. The potential of such an array for space weather observations has been studied using two techniques, namely Interplanetary Scintillations and Faraday Rotation. Both techniques depend on observing the emission from radio sources as they are occulted by a Coronal Mass Ejection traveling in the solar wind. The measurements will allow a determination of the density and velocity of the CME as well as its magnetic field strength and orientation. In addition, it will be possible to characterize the quiescent heliosphere and to study the variations in the Earths ionosphere on very small scales within the field-of-view of the array. This poster summarizes the array design, outlines the planned demonstrator system, and illustrates the expected heliospheric observations using simulations of recent space weather events.
This work was supported under NSF grants ATM-0317957and AST-0121164

8.8 SPI.08: Dependence of Equatorial Electron Densities on the Solar Soft X-Ray Flux – by Wang, Xiaoni

Status of First Author: Student in the poster competition PhD

Authors: Wang, Xiaoni Department of Electrical Engineering, University of Central Florida, Orlando, FL
Eastes, R. reastes@mail.ucf.edu Florida Space Institute, MS-FSI, Kennedy Space Center, FL 32899 United States
Bailey, S. University of Alaska, Geophysical Institute, Fairbanks, AK 99775
Valladares, C. Boston College, Inst Space Research, 140 Commonwealth Ave., Chestnut Hill,MA 02467
Woods, T. Univ. Colorado, Lab. Atmos. and Space Physics, 1234 Innovation Dr., Boulder,CO 80307

Abstract: Comparisons of short term variations in the soft X-ray data from the SNOE satellite and equatorial electron density data show excellent agreement. After removal of trends with periods longer than 27 days during undisturbed times (Ap less than 15), correlations of 0.6 are seen between the soft X-ray fluxes and the electron data. This is significantly better than the correlation, 0.4, found between F10.7 and the electron data. Both direct, changes in the ion production rate, and indirect, changes in the neutral density, effects contribute to the correlation between the solar fluxes and the electron data. Soft X-ray measurements from the SNOE satellite in wavelength bands of 2-7 nm, 6-19 nm and 17-20 nm have been compared with electron density data (TEC measurements from Ancon, Peru) for a period of almost three years. The excellent correlations observed indicate that even broad band measurements of the actual solar soft X-ray fluxes provide a significant increase in the accuracy of ionospheric predictions.

9 Wednesday Evening 30 June 2004 Poster Session Abstracts, Mesosphere and lower thermosphere gravity waves

9.1 GWV.01: Thermal Ducting and the ALOHA-93 Spectacular Gravity Wave Event – by Snively, Jonathan

Status of First Author: Student in the poster competition PhD

Authors: Jonathan B. Snively (jbs231@psu.edu), Victor P. Pasko (vpasko@psu.edu) **Abstract**: During the ALOHA-93 campaign, a particularly well-defined gravity wave train was observed in the OI and OH airglow emissions layers [Taylor et al., GRL, 22, 2849, 1995]. The observed waves had very short periods of approximately 4.4 minutes, with horizontal wavelengths of 20 kilometers. This observation was described as a spectacular gravity wave event as it exhibited several remarkable features. First, the observed waves had extraordinarily short periods suggesting that they could not have originated directly from a tropospheric source. Second, the waves were preceded by a well-defined and front-like enhancement of airglow emissions. Finally, the propagating waves appeared as opposite-phase perturbations of the OI and OH airglow emissions layers. Two explanations of the event have been proposed. The first is that the observed waves comprised a fully-ducted, multiple-node, gravity wave mode trapped between the upper mesosphere and lower thermosphere [Munasinghe et al., JGR, 103(D6), 6467, 1998]. The second explanation suggests that the observed waves were the result of a traveling undular bore, where a front-like disturbance excited a trail of waves as it dissipated and dispersed [Dewan and Picard, JGR, 103(D6), 6295, 1998]. However, neither explanation was found to be entirely satisfactory and no robust forcing mechanisms have been demonstrated. Here we revisit the wave-ducting interpretation of Munasinghe et al. [1998]. We first review classical ducting theory [Gossard and Hooke, Elsevier, p. 162, 1975] for a Doppler-shifted thermal duct, which perfectly explains the observed wave characteristics and velocities. We then present simulation results for a model atmosphere with conditions resembling those present on the night of the spectacular gravity wave event reported by Taylor et al. [1995]. The excitation mechanism we explore is that of Snively and Pasko [GRL, 30(24), 2254, doi:10.1029/2003GL018436, 2003], where the breaking of a tropospherically-generated gravity wave nonlinearly excites harmonic secondary waves at the altitude of the duct. Using steady-state models of OI and OH airglow emissions, we examine the applicability of this explanation to the observed phenomena.

9.2 GWV.02: Traveling Ionospheric Disturbance Characteristics Over Texas Using the TIDDBIT HF Doppler Radar – by Bronn, Justin

Status of First Author: Student in the poster competition Undergraduate

Authors: Bronn, Justin (Southwest Research Instititue, jbronn@swri.edu Crowley, Geoff (Southwest Research Instititue, gcrowley@swri.edu) Fessler, Brent (Southwest Research Instititue, bfessler@swri.edu) Wene, Greg (University of Texas at San Antonio, gwene@utsa.edu)

Abstract: Atmospheric gravity waves (AGW) are generated by numerous lower atmospheric processes, such as storms, and by auroral processes in the ionosphere. At ionospheric heights, the motion of the neutral gas in the AGW sets the ionosphere into motion. The waves displace the isoionic contours, resulting in a travelling ionospheric disturbance (TID). TIDs can be thought of as traveling corrugations in the ionosphere, and they can seriously affect HF radio communications and surveillance systems. Consequently, one of the most sensitive methods for detecting transient changes in the ionosphere is the HF Doppler technique operating in the 3-10 MHz band. A simple Doppler system consists of a CW (continuous wave) radio transmitter and receiver, which are highly frequency-stable. When a HF radio wave is reflected from the ionosphere, movement of the reflection point during passage of a TID produces a change in phase path and a Doppler shift proportional to the time rate of change of the phase path. The Doppler system is sensitive to motions of the ionospheric reflection point, and it therefore provides an accurate measure of both the TID and AGW periods. Similarly, because the TID velocity is determined simply from triangulation using the time-delays between perturbations at different reflection points, the

TID velocities are also an accurate estimate of the underlying gravity wave horizontal and vertical trace velocities. HF Doppler systems have advantages over all other techniques for the measurement of TID characteristics. They are more amenable to analysis than data from ionosonde chains, and their time resolution (30 sec) is much higher than that of ionosondes . Unlike total electron content (TEC) methods, which respond to height-integrated TID effects, the HF Doppler radar responds to TIDs at the altitude of the radio reflection point. Finally, HF Doppler systems have low power consumption, so that both spatial and temporal resolution can be maintained for many days without the costs that would be associated with an incoherent-scatter radar. SwRI recently designed, built and deployed an HF Doppler sounding system for three months, in Texas, to investigate TIDs. The TIDDBIT radar consisted of three transmitters (Austin, Uvalde and St. Hedwig) and a receiver in San Antonio, Texas. Using cross-spectral analysis and triangulation of the TIDDBIT signals, TID speeds and azimuths were obtained for each wave frequency. We provide a synoptic survey of the TID characteristics observed over Texas during January-March 2002. Such a system would be of great utility for the study of gravity wave seeding of low latitude ionospheric irregularities.

9.3 GWV.03: Simulation of Gravity Wave Perturbations of the F-Region – by Klenzing, Jeffrey

Status of First Author: Student in the poster competition PhD

Authors: J. H. Klenzing, University of Texas at Dallas, jeffk@utdallas.edu G. D. Earle, University of Texas at Dallas, earle@utdallas.edu S. G. Bateman, University of Texas at Dallas, shojinbat@yahoo.com

Abstract: We are developing a 2-D elementary numerical model of gravity wave perturbations in the F-region of the ionosphere, building on the work of Huang, et al. [JGR, 103, 6977, 1998]. Modifications to date include generalization to user-specified geographic locations, variations in production profiles, direct assimilation of MSIS neutral atmospheric data, and inclusion of realistic scale height variations. We are currently simulating both daytime and nighttime conditions for specific gravity wave k-vectors and amplitudes over Wallops Island, Virginia. These simulations can be compared to mid-latitude spread-F observed by the Wallops Digisonde. Our eventual goal is to simulate the E-F Coupled Layer Instability [Cosgrove, et al., preprint, 2003] in the nighttime ionosphere.

9.4 GWV.04: Climatology of Small-Scale Mesospheric Gravity Waves Observed over Antarctica – by Nielsen, Kim

Status of First Author: Student in the poster competition PhD

Authors: K. Nielsen, Utah State University, knielsen@cc.usu.edu M. J. Taylor, Utah State University, mtaylor@cc.usu.edu M. Jarvis, British Antarctic Survey

Abstract: As part of a collaborative research program between the British Antarctic Survey and Utah State University an all-sky CCD imager was deployed at Halley Station (75.5 S, 26.7 W), Antarctica and operated from April 2000 to September 2001. The primary goal of this investigation was the determination of the characteristics and sources of short period (less than 1 hour) gravity waves observed during the Antarctic winter in the absence of local tropospheric convection. In this study we have analyzed the spatial and temporal properties of 215 extensive wave events observed in the NIR OH emission (altitude 87 km), over two consecutive winter periods. The results show a clear tendency for poleward winter time propagation with a superposed east-west asymmetry that varies during the winter season. The azimuthal distribution and properties of these events will be discussed.

9.5 GWV.05: Statistical analysis of activity of medium-scale traveling ionospheric disturbances using IGS network – by Kotake, Nobuki

Status of First Author: Student in the poster competition PhD

Authors: Nobuki Kotake,kotake@stelab.nagoya-u.ac.jp, Yuichi Otsuka,otsuka@stelab.nagoya-u.ac.jp, Tadahiko Ogawa,ogawa@stelab.nagoya-u.ac.jp, Akinori Saito,saitoua@kugi.kyoto-u.ac.jp Takuya Tsugawa,tsugawa@stelab.nagoya-u.ac.jp

Abstract: Using GPS data taken from Geographical Survey Institute of Japan and International GPS Service, we investigate TEC perturbations associated with Medium-Scale Traveling Ionospheric Disturbances (MSTIDs). We use TEC data taken from five GPS receivers in each of six regions (Japan, South-California, East-America, South-America, Australia, and Europe). To reveal seasonal and local time variations of MSTID activity, ratio of standard deviation of TEC perturbation within one hour to background TEC is investigated. Statistical analysis using the TEC data in 1998, 2000, and 2001 shows that MSTID is most active in winter in the three years in the all regions. This result can be explained by a theory of Bristow et al. [1996] which tells that the lower probability of MSTID in summer may result from gravity wave reflection due to a steep temperature gradient with altitude below the cold summer mesopause.

9.6 GWV.06: Estimation of gravity-wave momentum flux from mesospheric airglow images – by Suzuki, Shin

Status of First Author: Student in the poster competition PhD

Authors: S. Suzuki [1],shin@stelab.nagoya-u.ac.jp, K. Shiokawa [1], shiokawa@stelab.nagoya-u.ac.jp, Y. Otsuka [1], otsuka@stelab.nagoya-u.ac.jp, T. Ogawa [1],ogawa@stelab.nagoya-u.ac.jp, T. Nakamura [2],nakamura@kurasc.kyoto-u.ac.jp, D. C. Fritts [3],dave@cora.nwra.com

Abstract: Gravity waves play important roles in both large- and small-scale dynamics of the atmosphere through their vertical transport of horizontal momentum fluxes. Wave dissipation causes divergence of momentum flux, which lead to local heating, turbulent diffusion, and accelerations of the local mean flow. Radar observations of gravity-wave momentum flux have been performed for the last few decades. However, the estimation of momentum flux from airglow images has been reported only recently. Here we estimated short-period gravity-wave momentum fluxes quantitatively from all-sky airglow images using the method proposed by Swenson and Liu [GRL, p.477, 1998]. Wave parameters required for this estimation were obtained from airglow images and simultaneous wind data. We used OH airglow images observed on November 13, 1999 at the Shigaraki MU observatory (34.9S, 136.1E). The mesospheric wind data were obtained by the MU radar. The observed gravity waves had horizontal wavelengths of 15-40 km, horizontal phase velocities of 20-100 m/s, and amplitudes of airglow intensity variance of 0.5-4%, which is estimated by two-dimensional FFT analysis. We found that 52% of the observed gravity waves were non-propagating waves (m2 is negative), suggesting evanescent or ducted waves, and do not transport momentum flux. The momentum fluxes transported by the freely propagating waves were estimated to be 1-20 m2s-2 with a mean value of 4.6 m2s-2. This value is comparable to the results reported previously using different approach to the OH airglow images and radar observations. In the presentation, we will also discuss the ambiguity of the estimation due to mixing of different waves in the airglow image and due to uncertainty of the Brunt-Vaisala frequency.

9.7 GWV.07: High Frequency Gravity Wave Momentum Flux Study Using Airglow Images at Maui, Hawaii – by Tang, Jing

Status of First Author: Student in the poster competition PhD

Authors: J. Tang, G. R. Swenson, A. Z. Liu, and F. Kamalabadi **Abstract**: A newly developed high frequency gravity wave momentum flux extraction method has been applied to airglow images and meteor radar winds taken simultaneously at Maui, HI (20.7N, 156.3W) during the Maui mesosphere and lower thermosphere (MALT) campaign. The method identifies individual quasi-monochromatic gravity waves with periods between 6 and 40 minutes, estimates the intrinsic wave parameters, and calculates the momentum fluxes carried by vertically propagating waves. Data taken in January, April, July, and October 2003 have been divided into summer and winter categories and nightly wave momentum fluxes are

calculated for seasonal comparison of wave propagation direction trends. In most of the April and July nights, the momentum fluxes were to the northeast while a southwest preference existed for the January and October nights. The results from Maui, HI, combined with the earlier results from other locations, support the notion that the seasonal trend in meridional flux is a global phenomenon.

9.8 GWV.08: Gravity Wave Calculations of an Unusual Mesospheric Bore Event Observed Over Antarctica – by Stockwell, R.

Status of First Author: Nonstudent

Authors: R.G. Stockwell (2), M.J. Taylor (1), K. Nielsen (1), R. H. Picard (3), M. Jarvis(4)
(1) Center for Atmospheric and Space Sciences, Utah State University, Logan, Utah, USA, (2) Colorado Research Associates, Boulder, CO, USA, (3) Air Force Research Laboratories, Hanscom AFB, MA,USA, (4) British Antarctic Survey, Cambridge, U.K.

Abstract: All-sky CCD observations of mesospheric gravity waves have been made from Halley Station Antarctica (75.5 S, 26.7 W) as part of a collaborative research program between British Antarctic Survey, U.K. and Utah State University, USA. A rare mesospheric bore event that was observed near-simultaneously in the nightglow emissions: over a period of several hours on the 27th of May, 2001. A preliminary local spatial spectra technique was applied to the images from an OH (87 km) nightglow imager. This analysis technique allows the measurement of group as well as phase velocity of the wave. Horizontal wavelength, observed frequency and observed horizontal phase velocity and the observed horizontal group velocity were recorded over several hours, allowing a look at the evolution of the wave packet. The wave group was seen to decelerate coinciding with a reduction in the wave packet's amplitude.

10 Wednesday Evening 30 June 2004 Poster Session Abstracts, Other waves (tidal, planetary, small scale, etc)

10.1 OWV.01: Local Spectral investigation of planetary waves in OH temperatures measured at Davis Antarctica. – by Stockwell, R.

Status of First Author: Nonstudent

Authors: R.G. Stockwell (1), G. B. Burns (2) , W.J.R.French (2)
(1) Colorado Research Associates, Boulder, CO, USA, (2)Space and Atmospheric Sciences,Australian Antarctic Division,Kingston,Tasmania,Australia

Abstract: Local spectral analysis of 7 years (1995-2001) of night-time hydroxyl (6-2)band rotational temperatures,measured with a scanning spectrometer over Davis station, Antarctica (68.6S,78,0E) was performed to search for long scale planetary wave oscillations. The analysis of several planetary wave type signatures which were observed over this long time period are presented.

10.2 OWV.02: Evolution of the polar mesopause during a Stratospheric Sudden Warming – by Bhattacharya, Yajnavalkya

Status of First Author: Student in the poster competition PhD

Authors: Yajnavalkya Bhattacharya, Dept. of Physics and Astronomy, York University, yajnaval at yorku.ca Dr. Gordon G. Shepherd, Centre for Research in Earth and Space Science, York University, gordon at yorku.ca

Abstract: A ground-based wide angle Michelson Interferometer was used to monitor the evolution of waves and airglow in the upper mesosphere and lower themosphere at Resolute Bay, Canada during a stratospheric warming event. Observed variability of zonal and meridional winds is compared to the temperature fields from assimilated stratospheric data. The time series of observed wind velocities is spectrally analyzed to show the evolution of waves of different periodicities and their amplitudes. Possible signatures of non-linear interactions between tidal, planetary and gravity waves is discussed.

10.3 OWV.03: Nonmigrating Tides over Antarctica using Space-Based and Ground-Based Wind Measurements – by Cierpik, K

Status of First Author: Student in the poster competition PhD

Authors: K. Cierpik University of Colorado, Boulder, Colorado cierpik@colorado.edu
J. Forbes University of Colorado, Boulder, Colorado forbes@colorado.edu
D. Murphy Australian Antarctic Division, Kingston, Tasmania, Australia
M. Tsutsumi, National Institute of Polar Research, Tokyo, Japan
D. Riggin, Colorado Research Associates/NWRA, Boulder, Colorado
R. Vincent, University of Adelaide, Adelaide, South Australia, Australia
S. Miyahara, Department of Earth and Planetary Science, Kyushu University, Fukuoka, Japan

Abstract: The combination of ground-based and space-based data to resolve tidal components is an important aspect of the TIMED mission. Herein, we demonstrate development of this capability using climatological winds from the UARS mission and five ground-based radars, and a specialized set of basis functions, to study summertime nonmigrating semidiurnal tides in the MLT region over Antarctica. Incorporating monthly-mean wind measurements from Davis, Mawson, McMurdo, Rothera and Syowa add to the temporal and spatial data grid created by combining multiple years of UARS data. It is theorized that by adding ground-based data, the aliasing and sampling problems faced by satellite data alone can be reduced. Moreover, the combined data plus the specialized basis functions lead to a model covering the whole Antarctic continent. To quantify these sources of error, the Kyushu University General Circulation

Model is sampled according to the UARS and ground station perspectives. The satellite-only and combined satellite/ground-based results are compared with results from a fully-sampled GCM database representing a true solution. Results from actual UARS data, collected over multiple years, combined with averaged ground-based data are presented using the GCM results for estimates of accuracy. Proposed future efforts using TIMED/TIDI data are outlined.

10.4 OWV.04: Jicamarca Radar Data Analysis and Comparison with GSWM for Tidal Components in the tropical mesosphere – by Guo, Liyu

Status of First Author: Student NOT in the poster competition Masters

Authors: Liyu Guo, Clemson University, lguo@clemson.edu Gerald Lehmacher, Clemson University, glehmac@clemson.edu

Abstract: Using the incoherent scatter radar (50 MHz) at Jicamarca (12.0S, 76.9W), the mesosphere was probed with 1 minute resolution. Radio wave scattering signals from the tropical mesosphere in January 1993, March 1994, and August 1994 during daytime were analyzed. The hourly averaged mean meridional wind for each day and each observation period were compared with the Global Scale Wave Model (GSWM). The comparison shows fairly strong tidal component in the radar data in August. The tidal component in Januarys data is indiscernible. The amplitudes of the radar data are on the same order of those of the GSWM data. The tidal component in March is not as strong as from the model, which maybe the result of other forms of dynamic processes balancing the tidal effect.

10.5 OWV.05: Semidiurnal tide observed in the polar mesosphere – by Iwahashi, Hiroyuki

Status of First Author: Student in the poster competition PhD

Authors: Hiroyuki Iwahashi, Nagoya University, iwahashi@stelab.nagoya-u.ac.jp; Satonori Nozawa, Nagoya University, nozawa@stelab.nagoya-u.ac.jp; Yasuhiro, Murayama, NICT, murayama@nict.go.jp; Masaki Tsutsumi, NIPR, tutumi@uap.nipr.ac.jp; Yasunobu Ogawa, Nagoya University, yogawa@stelab.nagoya-u.ac.jp; Ryoichi Fujii, Nagoya University, rfujii@stelab.nagoya-u.ac.jp **Abstract**: In order to understand effects of the upward propagating atmospheric waves onto background atmosphere in the mesosphere and lower thermosphere, we have investigated characteristics of atmospheric tidal waves in the polar mesosphere between 70 and 91 km using the wind data obtained with two MF radars located at the Tromsoe (69.58 deg N, 19.22 deg E) and the Poker Flat (65.1 deg N, 147.5 deg W).
We examined characteristics of semidiurnal tide based on MF radar wind data obtained from November 1998 to December 2002. We derived amplitudes and phases of two different semidiurnal tidal modes with zonal wave number 1 and 2. Observations at two sites make us possible to distinguish the two modes. Results are as follows: For semidiurnal tide with s=2, (1) At the all heights (88, 82, 76, 70 km), maximum amplitudes (10-25 m/s) are found in September. (2) The day-to-day variability of phase (local time of maximum) is very small (less than 2 hours) during summer and winter, but the difference of phase between summer and winter is large and close to 6 hours. (3) At the all heights, the phase values tend to shift towards earlier times with altitude increasing and the height profile of phase indicate the upward propagating waves.
For semidiurnal tide with s=1, (1) The seasonal variations are similar to semidiurnal tide with s=2, but the magnitudes are smaller (5-15 m/s). (2) At 88 km, the phase values are almost constant in summer, while the phase exhibits short-time (10-20 days) variation in winter. At 82, 76 km, the phase shows an intra seasonal variation (30-60 days) over the 4 years. At 70 km, the variation of phase values in equinox vary largely compared to those in summer and winter.
In this talk, we will report these results, and discuss the differences of these two modes. Furthermore, a possible wave-wave interaction between quasi 2day wave and semidiurnal tide will be discussed.

10.6 OWV.06: Tides Observed from both Ground-Based ERWIN and In-Orbit WINDII Instruments in High Latitude Mesopause Region – by Lee, Young-Sook

Status of First Author: Student in the poster competition PhD

Authors: Young-Sook Lee yslee@yorku.ca Gordon G. Shepherd gordon@yorku.ca
Centre for Research of Earth and Space Science (CRESS), York University, Toronto, Canada M3J 1P3

Abstract: Tidal oscillations of the mesopause region at northern high latitudes are investigated using WINDII (on UARS satellite) measurements of the horizontal wind velocity at about 96 km altitude from the observation of 557.7 nm O(1S) green line emission during March/93- April/97 and ERWIN observations of the same emission during Oct/95-Mar/97. A least-squares fit is performed to identify global migrating tidal waves in zonal mean winds from WINDII observations and in local ground-based ERWIN observations. The seasonal variation of semidiurnal tides observed at high latitude and at about 96 km has a minimum amplitude in summer and a maximum in fall, different from the summer maximum observed at the equator by McLandress et al.(1996). The meridional and zonal components of the zonal mean winds are superimposed on semidiurnal tides of large amplitudes of 14.4 m/s and 17.1 m/s respectively, compared with diurnal tides of small amplitudes of 3.8 m/s and 3.0 m/s, respectively, observed at 70 degrees latitude with a resolution of +/- 2.5 degrees. These dominant semidiurnal waves are interpreted as migrating tides based on both the consistency of maximum amplitudes fixed near the local times of 4-hr and 15-hr, and the reasonable agreement with a one hour difference with the semidiurnal oscillations seen in ground based ERWIN observations at +74.42 degrees latitude and 265.5 degrees longitude.

10.7 OWV.07: A simulation of 2-day Dynamo Induced Oscillations in the Ionosphere. – by Lichstein, Gilbert

Status of First Author: Student in the poster competition PhD

Authors: Gilbert Lichstein, University of Colorado, Boulder, lichstei@odo.colorado.edu Jeffrey Forbes, University of Colorado, Boulder

Abstract: 2-day oscillations have been observed in the F-region ionosphere. It has been suggested that these oscillations are caused by a 2-day planetary wave driving the ionospheric dynamo mechanism. Herein, we present the results of 3-D modeling efforts to verify this hypotheses.

10.8 OWV.08: Interannual Variability of Diurnal Tropospheric Heating and Diurnal Tides – by Lieberman, Ruth

Status of First Author: Nonstudent

Authors: Ruth S. Lieberman, Dennis M. Riggin and David A. Ortland

Abstract: We present analyses of tropospheric diurnal heating, and middle atmosphere diurnal tides. Our study highlights interannual variations, which have received comparatively little attention in the literature compared with seasonal studies. Analyses of 12 years of data from the Kauai MF radar and 8 years of data from the Christmas Island MF radar reveal significant interannual amplitude enhancements in the diurnal tide, particularly during 1992 and 1997. The amplitude maximum in 1997 is correlated with above-average tropical tidal heating due to IR absorption by water vapor. The tidal heating was derived using the NASA Water Vapor Project (NVAP) climatology. Examination of 10 years of monthly averaged tropospheric diurnal water vapor heating reveals an interannual component that maximizes over the Indian and tropical central Pacific oceans. This component explains over 40% of the total variance in the 10-year diurnal climatology of water vapor heating. Numerical experiments are currently in progress, to determine the MLT diurnal response to the variability in the water vapor forcing. We also explore the role of convective heating in modulating tropospheric diurnal forcing.

10.9 OWV.09: Searching for 6, 8, 12 and 24-hour Tides in six years (1998-2003) of Davis (68.6S, 78.0E), Antarctica, Hydroxyl Rotational Temperatures – by Burns, Gary presented by French, William

Status of First Author: Nonstudent

Authors: Gary B. Burns Australian Antarctic Division Kingston, Tasmania, Australia gary.burns@aad.gov.au
William J.R. French Australian Antarctic Division Kingston, Tasmania, Australia john.french@aad.gov.au

Abstract: Rotational temperatures from the hydroxyl (6-2) band have been collected at Davis station (68.6S, 78.0E), Antarctica, since 1998 with nominal 7 minute resolution. Hydroxyl emissions come from an 8 km wide layer near 87 km. Maximum diurnal coverage reaches 17 hours in mid-winter and exceeds 12 hours for the interval between April 25 (DoY 115) and August 13 (DoY 225).
Hydroxyl temperatures have been averaged into 30-minute bins centred on the UT hour and half-hour. Daily averages were subtracted from the half-hour values to reduce the influence of long-period variations, which can exceed 30 K over a 25-day period at this site. 31-day averages, at 5-day intervals, have been calculated to extract coherent tidal signals. A least-squares fit of combined 6, 8 and 12-hour sinusoids was used to determine the amplitude and phase of these tides. A 24-hour tidal fit was separately calculated, both with and without allowance for a temperature offset associated with the incomplete diurnal coverage. Typical tidal parameters were determined by two different methods to determine the coherency of the phase from year-to-year. Average values of the individual yearly amplitudes and phases were calculated for each 31-day interval. Separately, amplitude and phase values were determined for each 31-day interval after averaging the appropriate temperatures from all years.
The amplitude of the 6-hour tide occasionally exceeds 2 K, principally early in the winter or late in the winter. The phase of this tide is variable from year-to-year, except for early in the winter. Amplitudes of the 8-hour tide occasionally exceed 3 K in late winter, while the phase is relatively constant (maximising at 5, 13 and 21 UT +/- 2 hours). The 12-hour tidal amplitudes are generally of order 1 K early in winter, increasing to 2 K in late winter. The phases are somewhat variable from year-to-year in the early winter interval and more consistent (maximising at 3 and 15 UT +/- 3 hours) in mid- and late winter. Amplitudes of the 24-hour tide double relatively abruptly from 0.5 K to 1 K around mid-winter (from 1 K to 2 K if an offset is allowed). Phases of the 24-hour tide are consistent from year-to-year (9 UT +/- 3 hours).

10.10 OWV.10: Polar lower thermospheric wind dynamics based on EISCAT 8-day wind data obtained in November 2003 – by Nozawa, Satonori

Status of First Author: Nonstudent

Authors: Satonori Nozawa, Nagoya University, nozawa@stelab.nagoya-u.ac.jp; Sawako Maeda, Kyoto women's University, f54273@sakura.kudpc.kyoto-u.ac.jp; Takehiko Aso, NIPR, aso@nipr.ac.jp; Hiroyuki Iwahashi, iwahashi@stelab.nagoya-u.ac.jp; Yasunobu Ogawa, Nagoya University, yogawa@stelab.nagoya-u.ac.jp; Ryoichi Fujii, Nagoya University, rfujii@stelab.nagoya-u.ac.jp

Abstract: From November 11 to 19, 2003, the EISCAT UHF radar (so-called KST radar) and EISCAT Svalvard radar (ESR) were operated continuously with a Common Program two (CP2) mode which allows us to derive wind velocity vectors in the lower thermosphere (90-120 km). This campaign was made under collaborations of four countries such as Japan, Norway, Sweden and Germany. We conducted an EISCAT special program (SP) run for 66 hours with the KST radar and ESR followed by Common Program 2 to make 8-day window data set. Although the KST EISCAT radar has been under operation for about 20 years, this is the second 8-day long-run campaign followed by the 1999 July campaign. Aims of this campaign are as follows: (1) To investigate latitudinal variation of mean wind, and tidal winds. (2) To examine if quasi-2 day wave exists in the lower thermosphere in this time of year. (3) To investigate day-to-day variations of the semidiurnal wind amplitude. By using the data sets, we have derived mean winds as well as amplitudes and phase of quasi-2 day wave, diurnal tidal wind and semidiurnal tidal wind in Tromso (69.6 degree N) and Longyearbyen (78.1 degree N). We will present the results and discuss latitudinal variations of mean and tidal winds.

10.11 OWV.11: Observations and Modeling of the 6-Hour Tide – by Smith, Anne

Status of First Author: Nonstudent

Authors: Anne K Smith, ACD/NCAR, Boulder CO 80307 aksmith@ucar.edu
Dora V Pancheva, University of Bath, Bath UK eesdvp@bath.ac.uk
Nicholas J Mitchell, University of Bath, Bath UK n.j.mitchell@bath.ac.uk

Abstract: We present radar horizontal wind observations of the 6-hour tide over three years at Esrange (68N). This periodicity is a consistent feature in the wind variation. Its regularity and structure support the interpretation as tidal. A 6-hour tide is generated spontaneously in a 3-d numerical model. The model tide shares many features with that observed. Model results indicate that the tide is global, is generated primarily by solar heating, and is made up of migrating and non-migrating contributions.

10.12 OWV.12: TIDAL ANALYSIS OF MF RADAR DATA AT PLATTEVILLE, COLORADO – by Vemula, Sreenivas

Status of First Author: Student in the poster competition Masters

Authors: Sreenivas Vemula, UAF, ftsv@uaf.edu Dr.Denise Thorsen, UAF, ffdt@uaf.edu

Abstract: Abstract
We will present tidal analysis of MF Radar data collected at Platteville, Colorado (40.18 N, 104.7 W). This radar has been in operation since the summer of 2000 and we currently have three and a half years of 5-minute wind estimates at altitudes of 60 to 100 km. In this poster we will present our preliminary climatology of mean winds, tidal amplitudes and phases, as well as a comparison of time domain and spectral fitting routines.

10.13 OWV.13: Variations of atmospheric tides over the equator observed with Kototabang meteor radar, Sumatra, Indonesia (0S, 100E) – by Nakamura, Takuji

Status of First Author: Nonstudent

Authors: T. Nakamura(1), T. Tsuda(1), T. Djamaluddin(2), Suratno(2), A. Salatun (2) (1) Radio Science Center for Space and Atmosphere, Kyoto University, (2) National Institute of Aeronautics and Space of Indonesia nakamura@kurasc.kyoto-u.ac.jp/+81-774-31-8463

Abstract: As a part of CPEA (Coupling Processes in the Equatorial Atmosphere) project, RISH, Kyoto University and LAPAN, Indonesia started a meteor radar observation (37.7MHz) at the EAR (Equatorial Atmosphere Radar) site, Kototabang, West Sumatra, Indonesia in November 2002. The radar is located just on the equator, where the migrating S(1,1) mode is small, but various non-migrating modes are significant. In this study, diurnal, semidiurnal tides over West Sumatra are reported by using the observational data over one year. Short-time and long-time variations of tidal parameters will be focused.

11 Wednesday Evening 30 June 2004 Poster Session Abstracts, Mesosphere-lower thermosphere general studies

11.1 MLT.01: DWM: A global empirical model of disturbance winds in the F region – by Emmert, John

Status of First Author: Nonstudent

Authors: **Abstract**: Neutral winds are a key component of the coupled thermosphere-ionosphere system, and a solid understanding of them is therefore necessary for the interpretation and prediction of ionospheric phenomena, particularly during geomagnetically disturbed periods. The body of literature on thermospheric disturbance, or perturbation, winds (i.e., the change in the winds from their quiet-time patterns) is generally fragmented, with most studies focusing on data from a particular instrument or during a particular storm. The application of these results to the estimation of the global wind field is therefore limited. The most recent syntheses of upper thermospheric wind results, by Alan Hedin, were incorporated into successive versions of the Horizontal Wind Model (HWM-87, 90, 93), which are widely used for comparisons with other data and for input into theoretical ionospheric models. A weakness of HWM is that it does not accurately represent winds during geomagnetically disturbed periods, but since its last thermospheric update in 1991, an enormous number of new wind measurements have been made, and many advances have been made in our knowledge of storm-time dynamics.
We are currently constructing a global disturbance wind model (DWM) that will augment the HWM and which can be used independently as a scientific benchmark. We present a preliminary version of the model using perturbation winds derived from UARS-WINDII measurements. We also survey additional databases that will be studied and incorporated into the model, including the extensive FPI wind measurements contained in the CEDAR Database and satellite measurements by Dynamics Explorer 2 (DE-2) and Atmosphere Explorer-E (AE-E).

11.2 MLT.02: 3-D SPATIAL DISTRIBUTIONS OF MESOSPEHERIC OH (delta-v = 2) IR EMISSIONS OBSERVED FROM SABER – by Baker, Doran

Status of First Author: Nonstudent

Authors: D.J. Baker Utah State University spacegrant@cc.usu.edu
G.A. Ware Brigham Young University gene_ware@byu.edu
R.L. Fielding Utah State University rlfielding@cc.usu.edu

Abstract: Hydroxyl atmospheric gas, even though a minor species, nevertheless plays an important role in the dynamic energetics of the Earths atmosphere in the altitude region of the temperature mesopause. This is due to Meinel rotation-vibration band emissions. The NASA LaRC/USU SABER ten-channel Stirling-engine cooled radiometer aboard the LaRC/ JHU TIMED satellite globally monitors OH (delta-v = 2) emissions in two separate infrared channels centered at wavelengths of 1.65 and 2.06 m, respectively. The radiometer aboard the orbiting satellite employs a rocking mirror to give three-dimensional global coverage of the mesospheric OH emissions. Findings presented include graphical depictions of selected global distributions of partial OH band volume emission rates (VERs) and corresponding altitude at which peak VERs occurred. Graphical displays are presented for selected SABER observation days, including the intense solar storm of 4 November 2003 (UT 308).

11.3 MLT.03: Comparison of Czerny-Turner and Fourier Transform Spectrometer measurements of mesospheric OH temperatures. – by French, William

Status of First Author: Nonstudent

Authors: W. J. R. French Australian Antarctic Division Kingston, Tasmania, Australia john.french@aad.gov.au
G. B. Burns Australian Antarctic Division, Kingston, Tasmania, Australia gary.burns@aad.gov.au
R. P. Lowe University of Western Ontario, London, Ontario, Canada rlowe@uwo.ca

Abstract: A Fourier Transform Spectrometer (FTS, Bomem MR160LE) was installed at Davis station, Antarctica (68.6S, 78.0E) in Feb 2002 as an intended replacement for an aging Czerny-Turner Spectrometer (CTS, SPEX 1.26m f/9) which has measured emission lines in the OH(6-2) band, around 840 nm in 1990 and continuously since 1994.
Nocturnal hydroxyl airglow emissions originate from a layer about 8 km thick, centred near the mesopause at 87 km altitude. Rotational temperatures in the hydroxyl layer can be derived from measurement of the relative strengths of lines within hydroxyl emission bands. The FTS measures principally the OH(4-2) and (3-1) emission bands in the infrared region around 1.5 micron. Acquisition of spectra has increased by a factor of 4 with the new instrument, with two spectra (scan and flyback pairs) obtained every 4 minutes, compared to 7.5 minutes per spectrum for the CTS. Other benefits (eg. simultaneous spectral line sampling, extended diurnal and seasonal coverage and remote automated operation) and some disadvantages (eg. response calibration, detector noise) of the new system are discussed.
The co-located spectrometers have now operated concurrently for 2 years with an aim to ensure the continuity and consistency of a mesopause region temperature data set currently in its 12th year. Useful temperature comparisons can only be made after careful assessment of the instrument response calibrations, spectral line contamination, background subtraction and choice of transition probabilities. Experimental evidence, and a theoretical basis, shows some difference in temperature between vibrational bands. Upper vibrational states (v' = 6-9) are populated directly in the exothermic hydrogen-ozone reaction which produces excited OH, while lower states (v' less than 5) are populated via collisional quenching and radiative cascade. Deactivation of excited OH by atomic oxygen is also more efficient for lower vibrational levels than for higher. The altitude profile for lower vibrational levels, therefore peaks at lower altitudes. The difference is of the order of 3 km between v'=6 and v'=3.
Examples of nightly temperature variations derived from the two instruments, and nightly and monthly average temperature comparisons are presented and discussed.

11.4 MLT.04: Comparison of Derived Geostrophic Zonal Winds from TIMED/SABER and TIMED/TIDI Winds in the Mesosphere and Lower Thermosphere – by Criss, Adrienne

Status of First Author: Student in the poster competition Undergraduate

Authors: Adrienne E. Criss, E. R. Talaat, J.-H. Yee, J. M. Russell III, T. Killeen, M. Mlynczak, W. R. Skinner, L. Gordley, S. C. Solomon, Q. Wu **Abstract**: In this paper, we compare the winds derived from temperatures observed by the Sounding of the Atmosphere using Broadband Emission Radiometry (SABER) instrument onboard the Thermosphere Ionosphere Mesosphere Energetics and Dynamics (TIMED) temperatures to those observed by the TIMED Doppler Interferometer (TIDI) in the mesosphere and lower thermosphere region (70 105 km) using measurements from 2002 - 2003. SABER infers temperatures from 20 110 km on both the ascending and descending legs of the orbit. TIDI infers horizontal winds from 70 - 105 km using four telescopes, measuring four local times in the mid and low latitudes. Geostrophic and gradient winds are calculated from zonally averaged temperatures compiled for different time ranges: over spacecraft yaw cycles, seasons, and months. We will assess the accuracy of the geostrophic and gradient wind approximations in this region over the various time ranges.

11.5 MLT.05: Wind measurements in the Mesosphere/Lower thermosphere using the Platteville, CO MEDAC 50 MHz meteor radar. – by de la Pena, Santiago

Status of First Author: Student in the poster competition PhD

Authors: S. de la Pena, santiago.delapena@colorado.edu * S.K. Avery, susan.avery@colorado.edu * J.P. Avery, james.avery@colorado.edu* E.M. Lau, elias.lau@colorado.edu * D. Janches, diego.janches@colorado.edu* * Cooperative Institute of Research in Environmental Sciences

Abstract: Meteors falling into the earth atmosphere, at the rate of several thousands per day, leave a trail of ions that reflects electromagnetic waves. In the presence of a wind field, this trail drifts and causes a Doppler shift in the frequency of electromagnetic wave reflecting from it. This frequency shift, can be used to estimate the winds in the Mesosphere and Lower Thermosphere (MLT). The Meteor Detection and Collection (MEDAC) system described in this poster can be used as a receiving attachment to the Platteville, CO (40 N, 105 W) 50 MHz narrow-beam wind profiler or in conjunction with a new all-sky meteor radar system. In either transmitting configuration, MEDAC is currently using an improved five receiver interferometer in order to estimate the location of the trail, and record its Doppler frequency. Further processing yields mean wind estimations for the height range of 80 110 km. We present and discuss results of the meteor statistics and wind motions.

11.6 MLT.06: First 630 nm daytime and nighttime observations of thermospheric winds and temperatures with the Second Generation Optimized Fabry Perot Doppler Imager (SOFDI) – by Gerrard, Andrew

Status of First Author: Nonstudent

Authors: A. J. Gerrard, Clemson University, agerrar@clemson.edu J. W. Meriwether, Clemson University, john.meriwether@ces.clemson.edu

Abstract: The Second Generation Optimized Fabry Perot Doppler Imager (SOFDI), a state-of-the-art triple-etalon Fabry Perot interferometer with 4 independent field-of-views, has been successfully constructed and is now making initial observations of 630 nm OI emission in upstate New York during both day and night. In this paper we report on results from four different experiments. First, we present the results of a uninterrupted 48-hour calibration run which demonstrates the pressure and temperature stability of the system. Second, we show that SOFDI can make measurements of thermospheric winds with an accuracy of 15 m/s within 20 minutes for the daytime and 5 m/s within 5 minutes for the nighttime. Third, we report on nighttime observations of thermospheric vertical winds. Finally, we report the first recent observations of continuous 24-hour observations of thermospheric winds and temperatures, demonstrating SOFDIs daytime and nighttime observational capabilities. In conclusion, we highlight both 1) immediate scientific goals of the SOFDI instrument in combination with the Cornell all-sky imager and the MIT-Haystack optical observatory, and 2) long range plans which involve placement of the SOFDI observatory at the magnetic equator for measurements of equatorial winds and temperatures.

11.7 MLT.07: Interferometric Meteor Observations at the South Pole – by Lau, Elias

Status of First Author: Student in the poster competition PhD

Authors: Elias M. Lau, University of Colorado, CIRES, Elias.Lau@Colorado.EDU
Diego Janches, University of Colorado, CIRES, Diego.Janches@Colorado.EDU
Susan K. Avery, University of Colorado, CIRES, Susan.Avery@Colorado.EDU
James P. Avery, University of Colorado, Department of Electrical and Computer Engineering, James.Avery@Colorado.EDU
Scott E. Palo, University of Colorado, Department of Aerospace Engineering, Scott.Palo@Colorado.EDU
Nikolai A. Makarov, Institute for Experimental Meteorology, Scientific Production Association TYPHOON, Russia, makarov@obninsk.org

Abstract: Meteor radars estimate atmospheric winds in the Mesosphere/Lower Thermosphere (MLT) region by measuring the Doppler signature of the diffusing meteor trails. These trails are ionization columns created by the ablation of meteoroids that enter our upper atmosphere.

A meteor radar system was installed at the South Pole in 2001 to measure the horizontal wind field in the MLT region. It uses four 6-element yagi antennas pointing in orthogonal directions for transmission. For reception two independent systems are used: the same yagi antennas used for transmission (COBRA data acquisition system) and an interferometric array of five crossed-dipole antennas (MEDAC data acquisition system).
We present the results obtained using the interferometric receive array. Time, altitude, angular, and seasonal distributions of the observed meteors will be shown and discussed. Preliminary features of the observed wind field will also be presented and discussed relative to theoretical expectations and previous observations.

11.8 MLT.08: Validation of a new meteor radar system at South Pole – by Iimura, Hiroyuki

Status of First Author: Student in the poster competition PhD

Authors: H. Iimura, University of Colorado at Boulder, hiroyuki.iimura@odo.colorado.edu S. E. Palo, University of Colorado at Boulder, scott.palo@odo.colorado.edu Q. Wu, NCAR, qwu@ucar.edu

Abstract: The South Pole VHF meteor radar system is a quasi all-sky system designed to remotely measure the horizontal wind field in the mesosphere and lower thermosphere (MLT) region. This radar system was initially installed in January 2001 and became fully operational in January 2002. The radar operates at a frequency of 46.3MHz and transmits at a peak pulse power of 10kW. The system has the ability to determine the spatial location of meteor echoes given sufficient calibration. Using the estimated Doppler shift from the observed meteors and the assumptions that the meteors originate from an altitude of 93km and the vertical winds are negligible, one can estimate the horizontal velocity from an individual meteor echo. These observations are averaged over an hour to provide hourly estimates of the horizontal velocity. The TIMED spacecraft was launched in December 2001 and began science operations in January 2002. The TIMED Doppler Interferometer (TIDI) onboard TIMED has four telescopes. Each telescope has the capability to measure the line-of-sight direction horizontal wind. When a telescope directs towards the South Pole on every orbit it measures the horizontal wind field in the vicinity of the South Pole.TIDI wind data can be taken advantage of for the validation of meteor radar system. Because the meteor radar winds are two dimensional observations, with non-height resolution for this presentation, they can be projected to the TIDI telescope directions and compared with TIDI wind data. This presentation will introduce the meteor radar winds and give the statistical results of the comparison of TIDI and the meteor radar wind data for the seasonal and TIDI wind measurement altitude dependence.

11.9 MLT.09: On the variability of OH Meinel emissions observed by TIMED-SABER – by Marsh, Daniel

Status of First Author: Nonstudent

Authors: Daniel Marsh, ACD/NCAR, Boulder CO 80307 marsh@ucar.edu Anne K Smith, ACD/NCAR, Boulder CO 80307 aksmith@ucar.edu

Abstract: SABER, one of four instruments on board the TIMED satellite, observes the OH Meinel emission at 2.0 um that peaks near the mesopause. The emission results from reactions between members of the oxygen and hydrogen chemical families that can be significantly affected by mesopause dynamics. In this study we compare SABER measurements of OH Meinel emission rates and temperatures with predictions from a 3-dimensional chemical dynamical model. We describe the relative roles played by dynamical perturbations on OH emission, including the effects of tidal advection, and resulting density and temperature variations. The consequence of these variations on ground based observations is also examined.

11.10 MLT.10: Hand-waving through atmospheric general circulation with college physics – by She, Chiao-Yao

Status of First Author: Nonstudent

Authors: Chiao-Yao (Joe) She, Sean D. Harrell, Matthew L. James and David A. Krueger Physics Department, Colorado State University

Abstract: When first confronted by the counterintuitive thermal structure of the MLT (mesosphere and lower thermosphere) region, with winter warmer than summer, a beginning student (young or old) may be amazed with excitement and lost at the same time, without knowing where to turn. A quick trip to the library often ended up more buried under by the mathematics. It was indeed a pleasant surprise to the lead author when he discovered that it is possible to gain a conceptual appreciation of the mean temperature and horizontal wind structure of the atmosphere by hand-waving with the knowledge of college physics. This pedagogical poster will explain graphically (1) how solar heating leads to warm regions and pressure forces, (2) how the Coriolis effect balances the pressure force, producing zonal wind pattern in the troposphere and stratosphere solstices, (3) how are buoyancy waves with different phase velocities are filtered by zonal wind profiles, and (4) how the surviving waves break in the MLT, depositing momentum to alter the zonal wind direction and to induce pole-to-pole meridional flow, that cools and warms the MLT in summer and winter respectively. Lidar profiles will be used to verify the counterintuitive structures and to reveal some of the research challenges ahead.

11.11 MLT.11: USING HOUGH MODE EXTENSIONS FOR COMPARITIVE DATA ANALYSIS OF ATMOSPHERIC TIDES – by Svoboda, Aaron

Status of First Author: Student in the poster competition PhD

Authors: A. Svoboda, University of Colorado, aaron.svoboda@colorado.edu
J. Forbes, University of Colorado, Forbes@colorado.edu
S. Miyahara, Kyushu University, sbm@rossby.geo.kyushu-u.ac.jp

Abstract: Hough Mode Extensions (HMEs) are numerically-computed global modifications of Hough modes and velocity expansion functions that account for dissipative effects in the atmosphere. The dissipation results in modified vertical and latitudinal structures. In addition, the HMEs maintain global self-consistency in amplitude and phase between zonal and meridional winds, vertical wind, temperature and density. This feature can be exploited to make approximations in all height regimes from fitting local or sparse data. The HMEs are thus useful not only for comparing data in different regimes, but for estimating unobservable quantities such as density variability. We demonstrate the validity of using HMEs to extrapolate local data by implementing the procedure on output from the Kyushu general circulation model, whereby wind data in one height regime is used to make predictions of temperature in another. The method is then applied to wind data at 95 km from WINDII and HRDI on UARS, and predictions are compared to temperatures from UARS/MLS temperature data at 85 km. This comparison allows us to address the controversy surrounding the well-known net bias between ground-based and space-based winds in the 90-100 km altitude regime.

12 Wednesday Evening 30 June 2004 Poster Session Abstracts, LIDAR studies of the mesosphere-lower thermosphere

12.1 LID.01: Simultaneous observation of airglow structure with two imagers and a Na temperature-wind lidar, in Colorado – by Nakamura, Takuji

Status of First Author: Nonstudent

Authors: T. Nakamura (1), T. Fukushima (1), T. Tsuda (1), C.-Y. She (2), B. Williams (2), D. Krueger (2), W. Lyons (3) (1) Research Institute for Sustainable Humanosphere, Kyoto University, (2) Department of Physics, Colorado State University, (3) FMA Research, Inc
nakamura@kurasc.kyoto-u.ac.jp/+81-774-31-8463

Abstract: Ground-based airglow imaging has been used for observing dynamical features in the mesopause region such as gravity waves, bores, and instabilities. The observed structures are usually interpreted to be at the height of the center of typical airglow profiles, such as 87 km and 96 km for OH and OI(5577) images, respectively. However, recent satellite observations such as UARS/WINDII, HRDI have clarified that there are significant variations (more than a few km) in emission profile, as well as frequent occurrence of double peak emission profiles. The dual-site airglow imagings have also suggested a significant variation of the height of structures observed in the airglow images. Kyoto University and Colorado State University have started a collaborative observation of the structure heights in the OH airglow images with two all-sky imagers at Platteville (40.2N, 104.7W) and Yucca Ridge (40.7N, 104.9W) in Colorado. Winds and temperatures, as well as atmospheric stability are simultaneously observed with the Na temperature-wind lidar at Ft.Collins (40.6N, 105.1W). The estimated structure height in November 2003 was clearly affected by the existence of convectively unstable regions. Such an effect of atmospheric stability on the airglow image observations will be discussed in the paper.

12.2 LID.02: Current Status of ALOMAR-Webber Sodium Lidar Transmitter – by Acott, P.

Status of First Author: Student NOT in the poster competition PhD

Authors: P.E.Acott (CSU,acott@lamar.colostate.edu), J. D. Vance(CSU,vance@lamar.colostate.edu), B. P. Williams(CSU,biffw@lamar.colostate.edu), L. G. Su(UAF,ftls1@uaf.edu) and C.Y.She(CSU,joeshe@lamar.colostate.edu) **Abstract**: The ALOMAR-Webber sodium Lidar transmitter uses an innovative sum frequency generation (SFG) method to generate the continuous wave sodium light at 589nm to seed the transmitter of the lidar for simultaneous temperature, horizontal wind and sodium density measurements in the mesopause (80-110Km). After four years of operation, lessons have been learned as to the best way to operate this unique SFG system to improve: longevity, stability, and the accuracy of the data gathered. The poster will briefly describe the transmitter layout. The current SFG system with ion-beam-sputtered coatings on the resonator, deployed recently in March 2004, will be detailed with attention to the past problems that were encountered and how these problems were solved. A new containment system with a nitrogen purge combine with stricter controls regarding cleaning of the SFG crystal to ensure system longevity. New additions to the electronics allow for a more stable laser lock on the D2A peak, resulting in improved system stability. And changes in the way we sample the sodium spectrum yields greater resolution in frequency space making resulting data more accurate. These improvements combine to make the SFG a reliable and accurate solid-state solution for generating seed light for sodium lidar and other applications.

12.3 LID.03: Characteristics of Instabilities in the Mesopause Region over Maui, HI (20.7oN, 156.3oW) – by Li, Feng

Status of First Author: Student in the poster competition PhD

Authors: Feng Li, Alan Liu, Gary Swenson **Abstract**: Characteristics of instabilities in the mesopause region over Maui, HI are investigated using 20 nights, 130 hours of high-resolution wind and temperature data obtained by a Na wind/temperature lidar during the Maui-Mesosphere and Lower Thermosphere (Maui-MALA) campaigns. The mean probabilities for convective and dynamical instabilities are 3% and 10%, but with considerable night-to-night variations. A close linkage between instability and the Mesosphere Inversion Layers (MILs) in the mesopause region is found. Both convective and dynamical instabilities occur mostly in reduced static stability regions which are located above the MILs, with a tendency for dynamical instability to develop below convective instability. This particular structure is found to be closely related to the correlation of N2 and wind shear amplitude, which is identified for the first time in a statistical manner. The Maui-MALT data exhibit a distinct trend for N2 to increase with wind shear, and vice versa. It is found that the vertical variations of N2 are often highly correlated with those of wind shear with a phase shift such that the maximums and minimums of N2 are located 0.5-1 km below those of wind shear. Because of this shift, the decrease of N2 always leads the decrease of wind shear on the topside and above the strong wind shear layers. As a result, dynamical instability tends to develop in this region where small N2 is always associated with large wind shear. We also found that vertical shears in the horizontal wind are dominated by the contribution of the meridional wind, especially for those with large amplitudes. Possible mechanisms for the observed features are also discussed.

12.4 LID.04: Sodium Lidar Observed variability in mesopause region temperature and wind tides – by Li, Tao

Status of First Author: Student in the poster competition PhD

Authors: Tao Li, Colorado State University, taoli@lamar.colostate.edu Tao Yuan, Colorado State University, titus@lamar.colostate.edu Chao-Yao She, Colorado State University, joeshe@lamar.colostate.edu

Abstract: A 9-day continuous observation of the mesopause region temperature, zonal wind and meridional wind over Fort Collins, CO (40.6N, 105W) by the CSU two-beam Sodium Lidar between Sept. 21st and Sept. 29th, 2003 (UT day 264 to 272) makes it possible to study the tidal day-to-day variations. By performing the tidal fitting on a 24-hour continuous window centered at every 6-hour interval, time series of the semidiurnal tidal amplitudes and phases for the temperature, zonal and meridional winds were obtained. The results showed a dramatic day-to-day variation in amplitudes but much less change in phases. Lomb periodogram analysis on the 9-day continous dataset reveals, in addition to the expected strong diurnal and semidiurnal powers, quasi 3-day oscillations were present, particularly clear between 84km and 94km on the meridional wind spectrum, but less clear on the temperature and zonal wind spectra. The appearance of a 14hr component in the zonal and meriodional wind spectra suggests possible nonlinear interaction between the semidiurnal tide and a planetary wave with 3-day period. Further analysis on the day-to-day variations of the temperature and wind semidiurnal tide also shows a quasi 3-day modulation on the semidiurnal tidal amplitudes and phases. On the UT day 267, we also observed nearly 3-fold enhancement on the diurnal and semidiurnal amplitudes. Gravity wave variance (1.0 - 8hr period) on this day was also much larger in the same altitude range, 86-94km. The strong gravity wave activity is likely the cause for further enhancement on tidal amplitudes beyond the observed planetary wave modulation.

12.5 LID.05: SABER observations of CO2 concentration in the mesosphere and lower thermosphere and impact on SABER-lidar temperature comparisons at Fort Collins, CO. – by Mertens, Christopher

Status of First Author: Nonstudent

Authors: C. J. Mertens, NASA Langley Research Center, Hampton, Virginia (c.j.mertens@larc.nasa.gov) C.-Y. She, Colorado State University, Fort Collins, Coloroda (joeshe@lamar.colostate.edu) D.Siskind, Navel Reseach Laboratory, Washington, DC (siskind@uap2.nrl.navy.mil) M. Rapp, Leibniz Institute of Atmospheric Physics, Kuehlungsborn, Germany J. M. Russell III, Hampton University, Hampton, Virginia

(james.russell@hamptonu.edu) M. G. Mlynczak, NASA Langley Research Center, Hampton, Virginia (m.g.mlynczak@larc.nasa.gov)

Abstract: The Sounding of the Atmosphere using Broadband Emission Radiometry (SABER) experiment simultaneously retrieves kinetic temperature (Tk) and carbon dioxide (CO2) volume mixing ratio (vmr) in the mesosphere and lower thermosphere (MLT) from daytime measurements of CO2 15 um and CO2 4.3 um limb emission, respectively. At night SABER retrieves Tk from CO2 15 um limb radiance measurements and CO2 vmr is taken from the TIME-GCM climatology. We assess the quality of daytime-retrieved SABER CO2 concentrations by comparing nighttime SABER Tk profiles with Tk observations taken from sodium lidar measurements at Fort Collins, Colorado. We find that the SABER-lidar nighttime Tk comparisons are improved using SABER-retrieved CO2 profiles as compared to using the TIME-GCM CO2 climatological profile, bolstering confidence that SABER measurements are improving our knowledge of MLT CO2. Furthermore, we present zonal-average SABER CO2 data for various seasons and compare with TIME-GCM climatology. We initiate an assessment of the SABER-climatology CO2 vmr differences by studying the impact of eddy diffusion on model simulations of CO2 concentrations.

12.6 LID.06: Spectral Analysis of Temperature and Density Perturbations – by Nadakuditi, Sharma

Status of First Author: Student NOT in the poster competition Masters

Authors: Sharma Nadakuditi, University of Alaska Fairbanks, ftbn at uaf.edu

Abstract: The CRL-Rayleigh lidar observations yield temperature and density measurements in the stratosphere and mesosphere (40-80 km). Spectral and Statistical analysis techniques will be used to analyze the temperature or density fluctuations to characterize the wave activity in the stratosphere and mesosphere. This poster would aim at Weiyuans work by analyzing temperature as well as density profiles and compare the perturbations to determine the consistency in results.

12.7 LID.07: Comparison of Temperature Variations in the Earth's Mesopause – by Singleton, Tamara

Status of First Author: Student in the poster competition PhD

Authors: Tamara SingletoN Tulane University tsingl@math.tulane.edu

Abstract: The mesopause region of the Earth's atmosphere is characterized by abnormal seasonal temperature and large tidal variations. Scientists of the National Center for Atmospheric Research developed the Thermosphere-Ionosphere-Mesosphere-Electrodynamics General Circulation Model (TIME-GCM) in part to study the temperature variations in the mesopause. The TIME-GCM is a three-dimensional time-dependent simulation of the Earth's atmosphere that predicts winds, temperature, minor and major composition, and electrodynamics quantities globally from 30km to about 500km. Researches at Colorado State University (CSU) developed a sodium light and detection ranging instrument more than 10 years ago to examine and understand the nighttime temperature variability in the mesopause over Fort Collins, CO. In 2002 CSU extended the lidar capability to make daytime measurements enabling the determinations of diurnal mean, diurnal, and sub harmonic temperature variations between 80km and 100km. This research assessed the performance of the TIME-GCM by comparing the temperature variations taken from CSU's sodium lidar measurements of full diurnal cycles in the year 2002 with comparable TIME-GCM temperature predictions. Specifically, we studied and anlyzed the tidal components' amplitudes and phases using mathematical and computer applications to make comparisons and identify the strengths and weaknesses of the TIME-GCM with respect to depicting the sodium lidar observations.

12.8 LID.08: Heat Flux: A Case Study by Monte Carlo Statistic Method – by Su, Liguo

Status of First Author: Student in the poster competition PhD

Authors: Liguo Su and Richard L. Collins Department of Electrical and Computer Engineering, Geophysical Institute University of Alaska Fairbanks

Abstract: Abstract: We describe a novel Monte Carlo method for statistic analysis on Sodium Temperature/Wind Velocity Lidar measurements. The simulation results are obtained by simulating system error through combine pseudo noise with Lidar photon counts. In this poster, measuremental statistic features, such as RMS, Mean Value, Standard Deviation and Variance have been presented and discussed. We also demonstrate how to choose appropriate measurements specifications to do a robust Temperature or Wind Velocity measurement. This study is for single-layer-mesosphere analysis, Possion-like approximation by Gaussian distribution with a Mean Value much greater than 102. The histograms of retrieval temperature, wind velocity and heat flux show that under the same measuremental conditions, after different times of experiments, statistic features of errors caused by the system or ambient influence are different.

12.9 LID.09: Planetary waves and tides found using Lomb-Scargle periodogram analysis of Rayleigh-scatter lidar data above Utah State University – by Nelson, Karen presented by Wickwar, Vincent

Status of First Author: Student NOT in the poster competition Masters

Authors: Karen L. M. Nelson, Joshua P. Herron, and Vincent B. Wickwar Utah State University Center for Atmospheric and Space Sciences Logan, Utah 84322-4405 ddlsr@yahoo.com; jpherron@cc.usu.edu; vincent.wickwar@usu.edu

Abstract: Because of the significant gaps in nighttime-only data, traditional Fourier techniques are difficult to use to identify tides and short-period planetary waves. The Lomb-Scargle periodogram is a method that was developed by astronomers to identify oscillations in nighttime-only and otherwise incomplete data. For the same reasons, it is also a powerful tool for aeronomers. The Lomb-Scargle technique is described with particular emphasis on its application to nighttime-only lidar data. Because of the gaps in the data, attention is also placed on techniques used to identify aliasing in the Lomb-Scargle periodograms. The method is applied to temperatures from the Rayleigh-scatter lidar at Utah State Universitys Atmospheric Lidar Observatory (41.7N, 111.8W). It is applied to seven-day periods in both February, 1995, and August, 1995. In the winter period, in which the temperature profile is dominated by a large mesospheric inversion layer [Meriwether et al., 1998], the lidar data contain a quasi-5-day planetary wave and a 24-hr tide. In the summer period, the lidar data contain a quasi-5-day planetary wave at lower altitudes, possibly a quasi-2-day planetary wave at higher altitudes, and either 24-hour or 12-hour tides over much of the altitude region.

12.10 LID.10: Mesospheric Inversion Layers above Utah State University – by Thomas, Kristina presented by Wickwar, Vincent

Status of First Author: Student NOT in the poster competition Undergraduate

Authors: Kristina M. Thomas, Joshua P. Herron, and Vincent B. Wickwar Utah State University, Center for Atmospheric and Space Sciences, Logan, Utah 84322-4405 kmthomas@cc.usu.edu; jpherron@cc.usu.edu; vincent.wickwar@usu.edu

Abstract: A 10-year, mesospheric temperature climatology was produced using the Rayleigh-scatter lidar at the Atmospheric Lidar Observatory (ALO) at Utah State University (USU). Each of approximately 600 nights in this mid-latitude (41.7N, 111.8W) climatology was examined for mesospheric inversion layers

(MILs). Many of the MIL findings, in particular, the seasonal change in altitude, amplitude, and probability of occurrence are similar to those found at other mid-latitude locations. However, this detailed MIL analysis found several new results including a high probability of multiple inversions for a single profile, an increase in MIL amplitude with altitude, and little seasonal variation for large amplitude MILs.

12.11 LID.11: Mesospheric, Mid-latitude, Density Climatology above Utah State University – by Lundell, Eric M.

Status of First Author: Student in the poster competition Undergraduate

Authors: Eric M. Lundell and Vincent B. Wickwar Utah State University Center for Atmospheric and Space Sciences Logan, Utah 84322-4405 iamcire at yahoo.com vincent.wickwar at usu.edu

Abstract: Lidars have been used extensively to derive temperatures in the mesospheric region of the atmosphere. However, literature related to densities in the same region is relatively rare. A climatology of absolute densities between 45 and 90 km has been created using Rayleigh-scatter lidar observations. They produce relative density profiles that are then normalized at 45 km to an empirical model. The observations have been carried out since 1993 at the Atmospheric Lidar Observatory (ALO) at Utah State University (41.7N 111.8W). The climatology is based on 550 nights of data spanning a 10-year period. When normalized to the MSISe90 model, the climatology shows a large seasonal variation, with the summer densities in the 65-75 km region being approximately 50

12.12 LID.12: Variability and Trends in Mid-Latitude, Mesospheric Temperatures – by Wynn, Troy

Status of First Author: Student in the poster competition Masters

Authors: Troy A. Wynn (troywynn@cc.usu.edu), Joshua P. Herron (joshua.herron@usu.edu), and Vincent B. Wickwar (vincent.wickwar@usu.edu) Utah State University Center for Atmospheric and Space Sciences Logan, Utah 84322-4405

Abstract: The Utah State University Rayleigh-scatter lidar has provided mid-latitude (41.7N, 111.8W), mesospheric temperatures since late 1993. With this period approaching a solar cycle, a study has been initiated to examine the variability of the temperatures between 45 and 80 km, between September 1993 and July 2003. The temperatures have been analyzed using standard linear regression and optimization techniques to find contributions from the solar cycle, the annual and semiannual cycles, and a linear trend. The initial findings are presented and compared to those found by other groups.

12.13 LID.13: Another Noctilucet Cloud at 41.7 N – by Herron, Joshua

Status of First Author: Student in the poster competition PhD

Authors: Herron, Joshua P. Wickwar, Vincent B. Utah State University Center for Atmospheric and Space Sciences

Abstract: On June 22, 1995, a noctilucent cloud (NLC) was detected with the Rayleigh-scatter lidar at the Atmospheric Lidar Observatory (ALO) on the campus of Utah State University (USU) located in Logan, UT (41.7 N 111.8 W). This observation preceded, by four years, the one from 1999 that was previously reported [Wickwar et al., 2000]. These are both important because of their occurrence significantly equatorward of 50 latitude. The NLC was observed for 45 minutes shortly after local midnight. This was well past the twilight period when NLCs are visible to the naked eye. Several parameters of the NLC were measured by the lidar and are similar to those from the NLC observations in 1999. This NLC was approximately one km higher. Temperatures were measured in the surrounding region and found to be significantly cooler than the climatological mean.

12.14 LID.14: Atmospheric Lidar Observatory (ALO) Ten-Year Mesospheric Temperature Climatology – by Herron, Joshua

Status of First Author: Student in the poster competition PhD

Authors: Herron, Joshua P. joshua.herron@usu.edu Wickwar, Vincent B. vincent.wickwar@usu.edu Utah State Univerisity Center for Atmospheric and Space Sciences

Abstract: The Rayleigh-scatter lidar at the Atmospheric Lidar Observatory (ALO) on the Utah State University (USU) (41.7N, 111.8W) campus has been in operation since 1993. The temperature database now contains over ten years of Rayleigh-scatter temperatures. A muli-year temperature climatology has been calculated from these observations along with the RMS and interannual variability. These temperatures and the climatology are currently being used in a number of mesospheric studies, including mesospheric inversion layers, tides, planetary waves, cyclical variations, trends, longitudinal comparison, and validation studies.

12.15 LID.15: Anomalous behavior of mesopause region diurnal perturbations in winter temperature above Fort Collins, CO (105W, 40.5N) – by Yuan, Tao

Status of First Author: Student in the poster competition PhD

Authors: Tao Yuan and C. Y. She **Abstract**: CSU Na-Lidar system has been observing the mesopause above Fort Collins, CO (105B0W, 40.5B0N) over 20 months (Started in May 2002), on 24-hour continuous basis, weather permitting. These data sets, binned bimonthly, were used to study the seasonal variation of diurnal and semidiurnal tidal oscillation of temperature, zonal and meridional winds. We found excellent agreement between observation and Global Scale Wave Model predictions in diurnal tides, except in Nov-Dec period. The observed phase of temperature diurnal tide in Nov-Dec period of 2002, which showed trapping, is completely different from what models (GSWM and TIME-GCM) predicted. During the same period, however, the wind (zonal and meridional) diurnal tides are still basically following the models. The other winter period is Jan-Feb, 2003, in which the tidal behavior shows normal propagating mode and agrees well with model prediction. These observations are however in agreement with more recent data of Nov-Dec, 2003 and Jan-Feb, 2004. More amazingly, this 'anomalous' behavior in Nov-Dec was also found in earlier temperature only observation made in 1998-99. In this poster, we will show this winter anomaly in temperature diurnal tide in detail and present some possible explanations.

13 Wednesday Evening 30 June 2004 Poster Session Abstracts, Sprites and lightning

13.1 SPR.01: The initiation of carrot sprites – by Hiraki, Yasutaka

Status of First Author: Student in the poster competition PhD

Authors: Yasutaka Hiraki (Tohoku University, hira@pat.geophys.tohoku.ac.jp) and Hiroshi Fukunishi (Tohoku University, fuku@pat.geophys.tohoku.ac.jp)

Abstract: One of transient luminous events called as sprite sometimes exhibits a carrot-like shape. The carrot sprite is characterized by (1) onset of its optical emission with fine filamentary structures at an altitude of 70-75 km, which subsequently develops up-and-downward, and (2) larger delay time (5-150 ms) of its appearance from the onset of sferics, rather than that (around 1 ms) for other sprites (halo and column). It is suggested that electrical discharges in the lower ionosphere represent the upper (greater than 75 km) diffuse and lower (less than 75 km) streamer discharges. The fine structure of the carrot sprite is explainable as a streamer. The electrical breakdown for the carrot sprite is expected to start initially in the streamer region, not in the diffuse region. Using a quasi-electrostatic (QE) model, we investigate the parameter that lowers the altitude of breakdown onset far down to the streamer region. Result shows that the altitude is most dependent on the timescale of charge removal from thundercloud (lightning discharge). If the timescale is even large (tens of ms), the space-induced positive charges, which reflect the QE fields, are transported downward substantially. In the case, the QE fields slowly enhance and exceed the conventional breakdown field initially in the altitude of streamer region. The result can also explain the large delay time from sferics.

13.2 SPR.02: SOCRATES - Stratospheric Overflights of Convective Clouds Responsible for Atmospheric Transient Electric Fields Near Sprites – by Mende, Stephen

Status of First Author: Nonstudent

Authors: Stephen B. Mende, (mende@apollo.ssl.berkeley.edu) ,Harald U. Frey (hfrey@apollo.ssl.berkeley.edu), University of California, Berkeley, CA 94720, Robert Holzworth (bobholz@geops.geophys.washington.edu), Michael McCarthy (mccarthy@ess.washington.edu), University of Washington, Seattle, WA 98195 Walter Lyons (walyons@frii.com), FMA Research Inc. Fort Collins, Co 80524, Dave Klumpar (klump@physics.montana.edu), Montana State University, Bozeman, MT 59717-3840, ISUAL Colleagues

Abstract: The SOCRATES program is a focused effort to investigate the electrodynamics of Transient Luminous Events (TLEs), including sprites, halos and elves by making in situ electric field measurement in the vicinity of the TLE-s and simultaneously characterizing the TLE optical properties. The optical characterization will be augmented by the Imager of Sprites and Upper Atmospheric Lightning (ISUAL) observation on the Taiwanese ROCSAT-2 satellite. The measurement of the electric fields will be facilitated by electric field probes on low-cost meteorological sounding balloon payloads that will be launched into the stratosphere (30 km) above nocturnal mesoscale convective systems (MCSs). Mobile ground teams will be positioned to launch small (6 kg payload) balloons on the U.S. High Plains when sprite-producing positive cloud-to-ground lightning stokes (SP+CGs) are predicted. The key measurement will be the in situ vertical electric field component (Ez) in the immediate vicinity of SP+CGs. This will allow testing the predictions of various theoretical models of sprite formation. The balloon launch strategy is designed to overcome the considerable logistical problems which hampered prior attempts to place large-payload balloons over sprite producing storms. Multiple (4) ground stations will deploy low-light cameras (LLTVs) providing optical sprite confirmation and precise location via triangulation, thus overcoming another possible experiment coordination difficulty relating to poor visibility conditions at any single optical site. SOCRATES will greatly benefit from the first operational satellite-borne sprite imager

(PI: Rue-Ron Hsu, Taiwan) onboard ROCSAT-2. launched May 20th, 2004. ISUAL will provide the first routine, multispectral TLE images unhindered by atmospheric attenuation for comparison to ground-based sensors. SOCRATES will actively involve student teams in balloon launching, tracking and payload recovery activities. The SOCRATES campaign is envisaged to take place during the 2005 summer season.

13.3 SPR.03: Application of 3D FDTD Model of the Earth-Ionosphere Cavity to Studies of the Schumann Resonance Frequency Shifts During Solar Proton Events – by Yang, Heng

Status of First Author: Student in the poster competition PhD

Authors: Heng Yang, CSSL Laboratory, Pennsylvania State University, PA 16802, hxy149@psu.edu
Victor P. Pasko, CSSL Laboratory, Pennsylvania State University, PA 16802 vpasko@psu.edu

Abstract: The ground and the ionosphere can be considered as good electrical conductors at the extremely low frequency (ELF: 3-3000 Hz) and very low frequency (3-30 kHz), which form an electromagnetic cavity known as Earth-ionosphere cavity. The electromagnetic signals produced by the global lightning activity can propagate in this cavity and the lowest frequency components can travel around the Earth several times without serious degradation. The interference among these extremely low frequency signals produce resonances in the Earth-ionosphere cavity, called Schumann resonances [Schumann, Z. Naturforsch. A, 7, 149, 1952]. In this talk, a new three dimensional finite difference time domain (FDTD) model of the Earth-ionosphere cavity is presented. This model is designed for the simulation of the electromagnetic waves below 100 Hz propagating in the Earth-ionosphere cavity. The electron density and the geomagnetic field in the cavity are derived from the international reference ionosphere model (IRI) [Bilitza, Radio Sci., 36, 261, 2001] and international geomagnetic reference field model (IGRF) [Barton, J. Geomag. Geoelectr., 49, 123, 1997], respectively. The model accounts for a realistic latitudinal and longitudinal variation of ground conductivity (i.e., for the boundaries between oceans and continents) by employing a broadband surface impedance technique proposed in [Breggs et al., IEEE Trans. Antenna Propagat., 41, 118, 1993]. In this talk we will first compare the simulation results from our FDTD model with available analytical solutions and experimental measurements of the Schumann resonance frequencies. We will then discuss model changes of Schumann resonance frequencies under conditions of solar proton events (SPE) leading to substantial enhancements of the lower ionospheric electron density around the geomagnetic poles [e.g., Collis and Rietveld, Ann. Geophys., 8, 809, 1990]. We will provide comparisons of the model decreases in the first mode Schumann resonance frequency with corresponding changes recorded experimentally during SPE events [e.g., Schlegel and Fullekrug, JGR, 104, 10111, 1999; Roldugin at el., JGR, 108, 1103, 2003].

13.4 SPR.04: Characteristics of Transient Luminous Event Streamers in Weak Electric Fields – by Liu, Ningyu

Status of First Author: Student in the poster competition PhD

Authors: Ningyu Liu (nul105@psu.edu) and Victor P. Pasko (vpasko@psu.edu) CSSL Laboratory, The Pennsylvania State University, PA 16802

Abstract: It is well established by now that transient luminous events (TLEs) observed at different altitudes above thunderstorms commonly consist of large numbers of needle-shaped filaments of ionization, called streamers [e.g., Gerken and Inan, JASTP, 65, 567, 2003; Su et al., Nature, 423, 974, 2003; Pasko, Nature, 423, 927, 2003; and references cited therein]. We have recently developed a two-dimensional streamer model, which allows studies of the dynamics of streamers at various air pressures. Modeling results of double-headed streamers in strong electric fields E exceeding the conventional breakdown threshold field Ek, defined by the equality of the ionization and dissociative attachment coefficients in air, have been recently reported in [Liu and Pasko, JGR, 109, A04301, doi:10.1029/2003JA010064, 2004]. The study emphasizes importance of photoionization effects for understanding of observed propagation properties and branching of sprite streamers, and indicates that double-headed streamers originating from

single electron avalanches in lightning-driven quasi-static electric fields at mesospheric altitudes accelerate and expand, reaching transverse scales from tens to a few hundreds of meters and propagation speeds up to one tenth of the speed of light, in good agreement with recent telescopic [Gerken and Inan, JASTP, 65, 567, 2003], high-speed video [Stanley et al., GRL, 26, 3201-3204, 1999; Stenbaek-Nielsen et al., GRL, 27, 3829-3832, 2000; Moudry et al., JASTP, 65, 509-518, doi:10.1016/S1364-6826(02)00323-1, 2003] and multi-channel photometric [McHarg et al., JGR, 107(A11), 1364, doi:10.1029/2001JA000283, 2002] observations of sprites. The strong electric fields E¿Ek are needed for the initiation of streamers. The initiated streamers, however, are capable of propagating in fields substantially lower than Ek [e.g., Allen and Ghaffar, J. Phys. D: Appl. Phys., 28, 331-337, 1995], and one of the important questions of the current TLE research, which directly relates to the evaluation of the total volumes of atmosphere affected by the TLE phenomena and possible role of TLEs in establishing a direct path of electrical contact between the tropospheric and mesospheric/lower ionospheric regions, is related to the determination of the minimum electric fields (E .lt. Ek) required for the propagation of streamers in air at different pressures. In this talk, we will present our latest simulation results on propagation of streamers in weak (.lt. Ek) fields. The results indicate that the peak electric fields and electron densities of streamers in weak fields can be as low as 50% and 10% of those in strong fields, respectively. The velocities of streamers can drop down to as low as 100 km/s, which agree with those reported in existing streamer literature [e.g., Bazelyan and Raizer, Spark Discharge, 1998, p. 154] and with the observed speeds of vertical development of blue jets [e.g., Wescott et al., GRL, 22, 1209-1212, 1995; Pasko et al., Nature, 416, 152, 2002; Su et al., Nature, 423, 974, 2003]. At ground pressure, the decay of plasma in the streamer channel has been noticed in previous studies [e.g., Morrow and Lowke, J. Phys. D: Appl. Phys., 30, 614-627, 1997; Aleksandrov and Bazelyan, Plasma Sources Sci. Technol. 8, 285-294, 1999]. These observations have been attributed to the effects of three-body attachment and recombination processes, which are believed to be the major loss mechanisms of electrons in the streamer channel. In this talk we will discuss the effects of these two processes on streamer dynamics at low air pressures. We will also discuss the model determined minimum fields required for the propagation of streamers of different polarities at TLE altitudes.

Index